Universitat de Lleida

Modelling the energy dynamics of ventilated photovoltaic facades using stochastic differential equations in a monitored Test Reference Environment

Chiara Lodi

Dipòsit Legal: L.972-2012
http://hdl.handle.net/10803/84167

Universitat de Lleida

MODELLING THE ENERGY DYNAMICS OF VENTILATED PHOTOVOLTAIC FACADES USING STOCHASTIC DIFFERENTIAL EQUATIONS IN A MONITORED TEST REFERENCE ENVIRONMENT

CHIARA LODI

PhD Thesis

PhD Supervisors:

Dr. Daniel Chemisana Villegas

Dr. Joan Ignasi Rosell Urrutia

Departament de Medi Ambient i Ciències del Sòl

Universitat de Lleida

MODELLING THE ENERGY DYNAMICS OF VENTILATED PHOTOVOLTAIC FACADES USING STOCHASTIC DIFFERENTIAL EQUATIONS IN A MONITORED TEST REFERENCE ENVIRONMENT

CHIARA LODI

PhD Thesis

Presented in the

Departament de Medi Ambient i Ciències del Sòl

Universitat de Lleida

To obtain her Doctoral Degree

Lleida, May 2012

Acknowledgements

Agradecimiento a todas las personas que con su ayuda han colaborado en la realización del presente trabajo.

En particular, agradezco a mis directores de tesis, el Dr. Joan Ignasi Rosell y el Dr. Daniel Chemisana por el seguimiento, la motivación y el apoyo recibido a lo largo de estos años. En Lleida he encontrado un ambiente de trabajo excelente, siempre agradable y estimulante. Espero y deseo que la colaboración sigua también en el futuro.

Merece especial reconocimiento la orientación y la supervisión continua recibidas del Ing. Jordi Cipriano, que desde el principio ha creído en este trabajo y en mi. Le estoy sumamente agradecida y espero seguir colaborando en ocasiones futuras. El agradecimiento se extiende a CIMNE, en particular al BeeGroup, por el apoyo y los medios que he recibido a lo largo de estos años los cuales me han permitido desarrollar dignamente mi investigación.

Quisiera hacer extensiva mi gratitud a todos mis compañeros de trabajo del Departamento de Medi Ambient i Ciències del Sol, en particular George, Meredith, Chryssa, Amri, Carles, Gerard, Jerome, Noe, Bahy y Manel. Espero no perder nunca vuestra amistad y lealtad.

I would like to thank Mr. Hans Bloem from the European Commission DG JRC for his precious help and supervision during all the stages of my research work.

I would like to thank also Prof. Henrik Madsen, Peder Bacher, Philip Delff and all the members of the IMM Department of the DTU for their precious help in the modelling work and for the very friendly and nice stay that I had in their beautiful Denmark.

Un ringraziamento speciale per l'appoggio, la pazienza e l'affetto ricevuto dalla mia famiglia, dal mio ragazzo Alessandro e da tutti gli amici.

A todos ellos, muchas gracias.

Contents

Summary

Summary

The general aim of this work is to contribute to the energy dynamics assessment of mechanically ventilated double skin Building Integrated PhotoVoltaic (BIPV) systems under real outdoor weather conditions.

Mechanically ventilated double skin BIPV facades and roofs have gained increasing popularity in the past decade, especially for non-residential buildings. These building components appear as an attractive strategy for achieving the requirements of the last European Directives on the energy performance of buildings as they combine electricity generation with other functions of the building envelope. In order to achieve successful design solutions, building designers are interested in the performance under real operating conditions for a typical climate and specific location while taking into account the energy balance of their design.

Earlier work on this topic was examined and a lack of data on the actual performances of these systems and on the influence of different design parameters was found. Therefore, one of the objectives of this research work has consisted in collecting experimental data under real outdoor conditions. From the experience adquired in several research projects and the collaboration with the EC Joint Research Center of Ispra (Italy), an improved version of the Test Reference Environment (TRE) was designed and constructed at the Lleida Agri-food Science and Technology Park (PCiTal).

An extensive monitoring campaign has been carried out over a one year period. Several experiments, at different inclinations and ventilation regimes, have been performed. The electrical production and the temperature of the ventilated PV panel placed at the TRE have been compared with the performance of other two identical PV modules which represent respectively the worst and the best conditions: one reference module was fully insulated and the other one was left under free-rack conditions.

Based on selected experimental tests from the TRE, another goal was to estimate unknown physical parameters by using identification models. To achieve this goal, several stochastic grey-box models have been developed.

Special attention has been given to the identification of the heat transfer coefficients within the air cavity and the PV module heat capacity. The developed models have been correctly validated with several set of data from the experimental work at the TRE. The statistical evaluation of the two-state grey-box model has shown that the model properly describes the dynamics of the system.

Finally, from the experience gained during the experimental, analysis and modelling work, the definition of a standardized set-up for a Test Reference Environment for double skin applications of BIPV has been proposed.

Resumen

El objetivo general de este trabajo es contribuir a la evaluación de la transferencia de la energía en régimen dinámico de sistemas de doble piel FotoVoltaicos Integrados en Edificios (EIFV) con ventilación forzada bajo condiciones climáticas exteriores reales.

Las fachadas y los tejados de doble piel EIFV con ventilación forzada han ido aumentando cada vez más su popularidad en la última década, especialmente en edificios no residenciales. Estos componentes del edificio aparecen como una estrategia atractiva para lograr los requisitos de las últimas Directivas Europeas sobre la eficiencia energética de los edificios, ya que combinan la generación de electricidad con otras funciones de la envolvente del edificio. A fin de lograr soluciones constructivas exitosas, los diseñadores de los edificios están interesados en el comportamiento bajo condiciones reales de operación, para un clima típico y un lugar específico, teniendo en cuenta el balance energético de su configuración.

Los trabajos anteriores sobre esta temática fueron examinados y se detectó una falta de datos acerca de los comportamientos reales de estos sistemas y también de la influencia de los distintos parámetros de diseño. Por lo tanto, uno de los objetivos de este trabajo de investigación consistió en recolectar datos experimentales bajo condiciones externas reales. De la experiencia adquirida en varios proyectos de investigación y de la colaboración con el EC Joint Research Centre de Ispra (Italia), se diseñó y construyó una versión mejorada del "Test Reference Environment" (TRE) en el Parque Científico y Tecnológico Agroalimentario de Lleida (PCiTAL).

Durante un año se llevó a cabo una larga campaña de medidas. Se realizaron varios experimentos, con diferentes inclinaciones y regímenes de ventilación. La producción eléctrica y la temperatura del panel FV ventilado colocado en la TRE se compararon con las de otros dos módulos FV idénticos, los cuales representan, respectivamente, la peor y la mejor condición: un módulo de referencia fue totalmente aislado y el otro se dejó al aire libre.

Basado en una selección de datos experimentales provenientes del TRE, otro objetivo fue estimar parámetros físicos desconocidos mediante el uso de modelos de identificación. Para lograr este objetivo, varios modelos de caja gris estocásticos se desarrollaron.

Se prestó particular atención a la determinación de los coeficientes de transferencia de calor en el canal de aire y de la capacidad térmica de los módulos FV. Los modelos desarrollados se validaron correctamente con varias series de datos provenientes del trabajo experimental en el TRE. La evaluación estadística del modelo de caja gris de doble estado ha demostrado que el modelo describe adecuadamente la dinámica del sistema.

Por último, a partir de la experiencia adquirida durante el trabajo experimental, de análisis y de modelación, se ha propuesto la definición de un entorno de prueba "Test Reference Environment" estandarizado para las aplicaciones de EIFV de doble piel.

Resum

L'objectiu general d'aquest treball és contribuir a l'avaluació de la transferència de l'energia en règim dinàmic de sistemes Fotovoltaics de doble pell Integrats en Edificis (EIFV) amb ventilació forçada sota condicions climàtiques exteriors reals.

Les façanes i les teulades de doble pell EIFV amb ventilació forçada han anat augmentant cada vegada més la seva popularitat en l'última dècada, especialment en edificis no residencials. Aquests components de l'edifici apareixen com una estratègia atractiva per aconseguir els requisits de les últimes Directives Europees sobre l'eficiència energètica dels edificis, ja que combinen la generació d'electricitat amb altres funcions de l'envolupant de l'edifici. A fi d'aconseguir solucions de disseny reeixides, els dissenyadors dels edificis estan interessats en el comportament sota condicions reals d'operació, per a un clima típic i un lloc específic tenint en compte el balanç energètic de la seva configuració.

Els treballs anteriors sobre aquesta temàtica van ser examinats i es va detectar una falta de dades sobre els comportaments reals d'aquests sistemes i també de la influència dels diferents paràmetres de disseny. Per tant, un dels objectius d'aquest treball de recerca va consistir a recol.lectar dades experimentals sota condicions externes reals. De l'experiència adquirida en diversos projectes d'investigació i de la col.laboració amb el EC Joint Research Center de Ispra (Itàlia), es va dissenyar i construir una versió millorada del "Test Reference Environment" (TRE) al Parc Científic i Tecnològic Agroalimentari de Lleida (PCiTAL).

Durant un any es va dur a terme una llarga campanya de mesures. Es van realitzar diversos experiments, amb diferents inclinacions i règims de ventilació. La producció elèctrica i la temperatura del panell FV ventilat col.locat en el TRE van ser comparats amb les d'altres dos mòduls FV idèntics, els quals representen, respectivament, la pitjor i la millor condició: un mòdul de referència va ser totalment aïllat i l'altre es va deixar a l'aire lliure.

Basat en una selecció de dades experimentals provinents del TRE, un altre objectiu va ser estimar paràmetres físics desconeguts mitjançant l'ús de models d'identificació. Per aconseguir aquest objectiu, diversos models de caixa grisa estocàstics es van desenvolupar.

Es va prestar particular atenció a la determinació dels coeficients de transferència de calor al canal d'aire i de la capacitat tèrmica dels mòduls FV. Els models desenvolupats van estar correctament validats amb diverses sèries de dades provinents del treball experimental en el TRE. L'avaluació estadística del model de caixa grisa de doble estat ha demostrat que el model descriu adequadament la dinàmica del sistema.

Finalment, a partir de l'experiència adquirida durant el treball experimental, d'anàlisi i de modelatge, s'ha proposat la definició d'un entorn de prova "Test Reference Environment" estandarditzat per a les aplicacions de EIFV de doble pell.

Chapter 1: Introduction and objectives

Introduction and objectives

Abstract

The introduction presents and discusses the main topics of the research work. The framework, objectives and structure of the Thesis are presented. The manuscript-based Thesis is structured as a collection of papers, two of them are published in international peer-reviewed journals while the other two are to be submitted for publication.

1. Framework of the thesis

Energy plays a fundamental role in determining a country's level of economic development. Since the 1980s an intensive set of legislative regulation has been implemented in Europe relating to energy issues. The reasons for this increasing interest in energy regulation are to be found in increases in industrial production, energy consumption and environmental protection.

Over the last 20 years, interest in renewable energy has strongly increased. In 1997, the European Commission adopted a White Paper [1] for a Community Strategy and Action Plan concerning the future of renewable energy in the European Union. The White Paper set a target of doubling renewable energy use by 2010 (from 6 % of total consumption in 1996 to 12 % in 2010). Under the Kyoto protocol [2], the European Union has committed itself to reducing the emissions of greenhouse gases by 8 % in 2012 with respect to the level in 1990. The need to increase energy efficiency and renewable energies is part of the triple goal of the '20-20-20' European initiative for 2020 [3], which means a saving of 20% of the Union's primary energy consumption and greenhouse gas emissions, as well as the inclusion of 20% of renewable energies in energy consumption.

Energy consumption in residential and commercial buildings represents around 40 % of the total energy used in the European Union and it is responsible for 36% of the European Union's total CO_2 emissions. Therefore, the reduction of energy consumption and the use of energy from renewable sources in the building sector constitute important measures which are needed to reduce the Union's energy dependency and greenhouse gas emissions. Renewable energies in the building sector have to be promoted for achieving the requirements of the European Directive 2002/91/EC on the energy performance of buildings (EPBD) [4], and the new recast of the directive [5], in particular for supporting the design of nearly-zero energy buildings (NZEB).

One of the most promising renewable energy technologies is photovoltaic (PV) technology and Building Integrated Photovoltaic (BIPV) systems have been widely developed in the past decade. PV cells operation is based on the ability of semi-conductors to convert sunlight into electricity by exploiting the *photovoltaic effect*. Commercially available photovoltaic elements only allow transforming up to approximately 18 % (mono-crystalline silicon) of the incident solar radiation into

electrical energy. The remaining incident solar radiation is converted into sensible heat, which results in the warming-up of the PV elements. Since the relative temperature coefficient of crystalline silicon PV cells is in the range of 0.4-0.6%/K, an increase in temperature leads to a reduction in the PV electrical efficiency. By ventilating the rear surface of the PV module, the heat transfer rate increases, thus reducing the PV cells temperature and increasing their electrical conversion efficiency. Therefore, an attractive concept is the integration of the PV systems in buildings as double skin ventilated facades or roofs and the use of the pre-heated air within the ventilated air gap. This approach combines electricity generation with other functions of the building envelope. In fact, apart from increasing the electrical efficiency of the system, the pre-heated air may reduce the ventilation thermal losses and the heating demand of the building. In addition, the ventilated façade might be coupled with the heating and ventilation air-conditioning (HVAC) system of the building, increasing its efficiency.

Since the implementation of the EPBD and the EN 13779 [6] directives has fixed considerable air renovations per hour for non-residential buildings, ventilated BIPV systems might reduce these ventilation thermal losses by pre-heating the fresh air. Since mechanical ventilation systems are normally installed in non-residential buildings, this research work is focused on forced ventilation regimes within the air cavity.

Semi-transparent BIPV facades or roofs are a promising application as a certain degree of natural daylighting is allowed. For this particular application, the PV laminate is usually composed of two layers of highly transparent glass sheets, and a series of opaque PV cells that are encapsulated in between. One of the glass sheets may be substituted by transparent Tedlar. By increasing the solar cells area of semi-transparent BIPV modules, the electricity production increases while solar heat gain and daylight utilization are reduced. Therefore, a balance should be made between these factors for each particular case.

The integration of BIPV modules in the building envelope is actually determined by their high-tech appearance and by the favorable feed-in tariff scheme implemented by some European countries. Although, as in the case of Spain, there is a higher economic incentive for building integrated photovoltaics (BIPV) than for land based PV installations, this difference is not enough to balance the harmful effects of the architectural integration. Therefore, the effective use of the generated heat at the vertical air gap constitutes a crucial issue for the economic viability of these complex facades.

Building designers are interested in the performance under operating conditions for a typical climate and location taking into account the energy use of their design. A further consideration is that building designers need performance indicators based on climatic variables: ambient temperature, solar radiation, wind velocity and site dependent data such as obstructions giving possible shading problems.

PV components, integrated in a building's envelope, interact with the building in many respects (see Fig. 1). A comprehensive assessment procedure should include the following aspects:

- Electrical performance;
- Thermal processes at component level;

- Seasonal dependency of the thermal performance;
- Ventilation performance;
- Visual performance;
- Maintenance related aspects and durability;
- Other performance objectives.

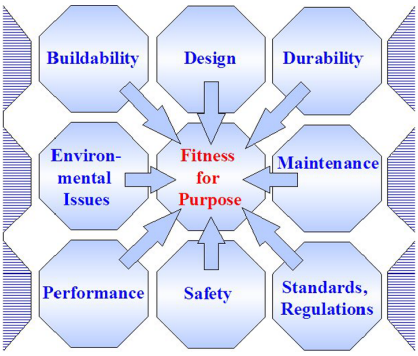

Figure 1: Schematic presentation of different aspects for PV building integration [7]

The technical data provided by the PV industry are based on standardised measurements under laboratory conditions described in IEC 61215. The most important test procedures are:

- 10.2 Standard Test Conditions (STC),
- 10.5 Measurement of Nominal Operating Cell Temperature (NOCT),
- 10.6 Performance at NOCT,
- 10.7 Performance at low irradiance.

Concerning 10.5, NOCT is defined as the equilibrium mean solar cell junction temperature within an open-rack mounted module in the following Standard Reference Environment (SRE):

- Tilt angle: at normal incidence to the direct solar beam at local solar noon
- Total irradiance: 800 W/m^2
- Ambient temperature: 20 °C
- Wind speed: 1 m/s
- Electrical load: 0 A (open circuit, thus no current flowing)
- Open rack mounted PV modules with optimised inclination.

A number of different circumstances occur when PV modules are applied as integrated components in a building, which is far from the Standard Reference Environment as described in the IEC 61215: the inclination for façade application is typically 90°, and for roof applications it depends on the roof construction but is seldom optimised and free convection at the rear side of the PV modules does not occur. The most notable differences are in level of irradiation and operating cell temperature. Therefore, conversion from PV module specifications at Standard Test Conditions to BIPV applicable electric system design values is of highest priority.

Double skin BIPV applications require a careful study of their energy characteristics. The convective heat transfer within the air cavity is the most complex part of the thermal process. In

fact, this heat transfer process involves a combination of forced and natural convection, laminar and turbulent flow and, at least in the entrance sections, developing flow (where the hydrodynamic and thermal flow profiles are both evolving).

In recent years, several authors have been working on the energy characterization of double skin ventilated systems, both with and without integrated PV systems. In literature it is possible to find several studies on ventilated transparent double skin applications (see [8, 9, 10, 11]) while only a few authors have focused on ventilated double skin BIPV systems (see Chapter 2). Several European projects have focused on the energy dynamics characterization of these building components: starting from the first EC PASSYS projects [12] (1986-1994), it was found that BIPV system evaluation requires the combination of well-controlled experimental measurements under real climatic conditions with detailed simulation techniques. The following EC PV-HYBRID-PAS project [13] (1994–1998) was aimed at developing standardised test procedures for the overall energy performance evaluation of hybrid PV building components. Tests on hybrid PV components were carried out with both natural and forced ventilation using PASLINK test cells (see Fig. 3) located in several different climates. One of the conclusions drawn from this project was that outdoor measurements of the energy balance must be performed under well-described and controlled conditions in order to use the data to calibrate numerical models. The need for well-described and standardised testing conditions was the core issue of the EC PRESCRIPT project [14] (1997–1999) regarding the development and benchmarking of a pre-standard for testing PV roofs and facades. In the context of this European project it was emphasised that standard test procedures, as described in IEC 61215, are not directly applicable for BIPV systems.

Several laboratory tests were carried out to evaluate the energy performance of double skin BIPV systems (see [15, 16]). These tests are normally accurate and replicable, however, they are unable to replicate real climate effects and in general they do not take into account the dynamic variations in the boundary conditions of the component integrated into a real building. On the other hand, experiences involving the measurements of real buildings (see [17, 18, 19]) revealed that these studies are expensive and fraught with several problems, such as those related to achieving good quality data, isolating the performance of the individual components, and extending results to different buildings, occupancies and climates.

In Fig.2 examples of full-scale double skin BIPV applications in occupied buildings are presented. An early example of monitored full-scale ventilated PV façade is the public library at Mataró near Barcelona [17]. This ventilated PV façade has been studied in a series of European projects [20]: the façade is 6 meters high by 37.5 m wide and it is composed by 20 kWp multi-crystalline glass-glass PV modules with a 14 cm ventilation air gap.

Figure 2: Full-scale double skin BIPV facades. (a) Public Library of Mataró, Spain; (b) Paul Horn Arena in Tübingen, Germany; (c) Central Railroad Station in Freiburg, Germany; (d) The apartment building in Skovlunde, Denmark

Considering the limitations of both laboratory tests and monitoring of real occupied buildings, several authors have therefore considered outdoor test facilities as economical and practical intermediate bridges. In outdoor test environments, real climate effects are taken into account and a high degree of indoor environment control is reached, avoiding occupancy effects, so that these systems can serve as a good compromise between laboratory and full-scale building testing.

Several aspects are considered for the experimental work carried out in outdoor tests facilities:

- identification of the information needed to derive the required characteristics;

- choice of the type and number of the sensors (accuracy, costs, etc.);

- positioning of the sensors (protections, etc.);

- definition of the measurements logging period and the extension of the monitoring campaign (duration of the tests period, etc.)

In literature, several test facilities have been used for monitoring mechanically ventilated transparent double skin facades. Relevant examples are the outdoor test stand at the Mechanical Engineering Faculty Building of the Technical University of Munich in Garching [9], the TWINS (Testing Window Innovative Systems) test facility at the Department of Energetics of the Politecnico di Torino [11] and the Vliet test building of the Laboratory of Building Physics in Leuven [10] (see Fig. 3).

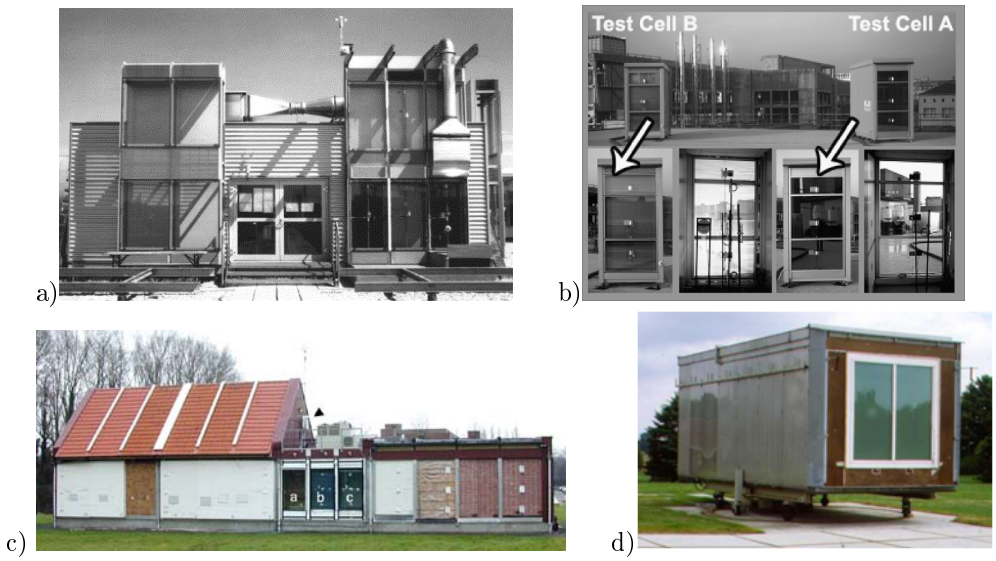

Figure 3: Outdoor test facilities for transparent double skin applications. (a) Outdoor test stand at the Technical University of Munich in Garching, Germany [9]; (b) TWINS at the Politecnico di Torino, Italy [11]; (c) Vliet test building of the Laboratory of Building Physics in Leuven, Belgium [10]; (d) Paslink test cell at the Belgian Building Research Institute of Limelette, Belgium [21]

However, only a few outdoor test facilities have been used for testing double skin BIPV systems. During the EC IMPACT project [22] (1998–2000), the first version of an outdoor Test Reference Environment (TRE) (see Fig.4) for double skin applications of BIPV systems was built at the EC Join Research Centre (JRC) of Ispra [23]. The purpose of the experimental work on the TRE was to obtain several data series for the same PV module under different boundary conditions and to compare them with data series from other PV modules. Different experiments were carried out within the first TRE set-up, testing different PV module compositions under several air flow rates and studying the effect of aluminium transversal fins of 5 cm length over the air gap rear-facing surface.

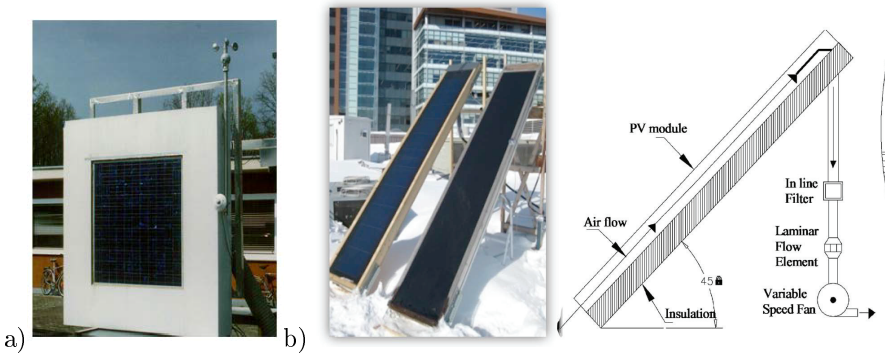

Figure 4: (a) Test Reference Environment for double skin BIPV systems at the EC JRC of Ispra, Italy; (b) Experimental set-up for testing ventilated BIPV systems at the Concordia University (Canada)

Reference mini-modules were specifically designed during this project, for testing the performance of similar PV module composition in fully insulated and free-rack conditions [24]. Another example of experimental set-up for testing ventilated BIPV systems is the experimental set-up for testing ventilated BIPV systems at the Concordia University in Canada (see Fig.4).

A well designed and equipped test facility is fundamental in order to achieve high quality data for the characterization of the energy dynamics of the building component.

Several approaches to the analysis and modelling work of double skin BIPV system are present in literature (see Chapter 2).

Based on high quality experimental data, mathematical evaluation techniques have been applied in literature to identify unknown parameters by means of comparing measured and modelled data.

A dynamic system can be schematically represented as in Fig. 5. The system has a number of input variables, u(t), it is affected by the disturbances v(t), and it has output signals y(t). The output signals are measured variables, which provide useful information about the system. For a dynamic system the control action at time t will influence the output at future time instants.

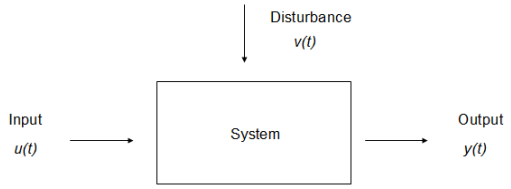

Figure 5: Schematic representation of a dynamic system

The models are the mathematical descriptions of the systems and they are needed for the analysis, prediction and design of the dynamic systems. They are by definition simplifications of reality. There are two ways of constructing mathematical models [25]:

- Mathematical modelling: an analytical approach, where the dynamic behaviour of a phenomena or a process is described with basic laws from physics;

- System identification: an experimental approach, where some experiments are performed on the system and a model is fitted to the input data by identifying suitable values to its parameters.

System identification is applied throughout the following steps [26]:

1. An experiment is performed by exciting the system and regular observing its input and output signals over a time interval;

2. Input and output signals are recorded for subsequent "information processing";

3. A parametric model is developed to process the recorded input and output sequences (several models can be applied);

4. An appropriate form of the model is determined, typically a linear differential equation of a certain order;

5. A statistically based method is used to estimate the unknown parameters of the model.

Applying system identification on physical system, knowledge about the system is required at all stages. The goal is to estimate physical parameters by using identification models.

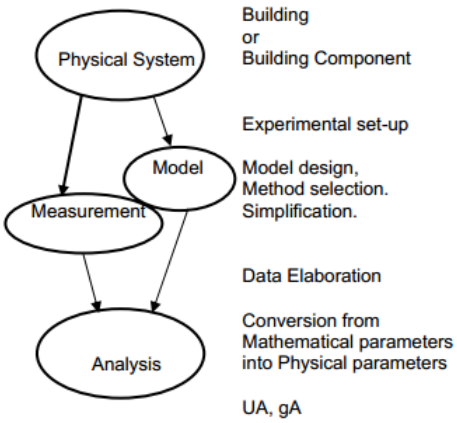

Figure 6: Overview of system identification steps [26]

The following six points can be distinguished in the general approach of solving the problem of energy performance assessment using identification techniques:

1. Design the experiment: in a first phase the experiment must be designed taking into account the objective and all available physical knowledge;

2. Perform the experiment and collect data: the duration of the experiment must be long enough to fulfill all objectives;

3. Pre-processing: check for irregularities by having a global look at the data, e.g. by plotting some of the important input signals and to examine statistical information of the data;

4. Analysis by estimation: choose and apply a model and method;

5. Post-processing of the results:

    1. Fit to the data (residuals that behave as white noise);

2. Reliability, in order to obtain the same results with different data;
3. Internal validity, e.g. cross-validation;
4. External validity, to check if results are in general not in conflict with previous experience;
5. Dynamic stability;
6. Identifiability, to verify that the model's parameters are uniquely determined by the data
7. Simplicity, in order to get the minimum number of parameters and simplify the conversion from mathematical parameters into the required physical ones. This has often been found as cause for problems, misunderstanding and errors.

In general two types of criteria for parameter identification can be distinguished: the Prediction Error Method (PEM) and the Output Error Method (OEM).

The Prediction Error Method (PEM) is based on statistical models to find parameters by minimising the error between a k-step (usually k=1) ahead prediction and the measured output. Some characteristics are:

- more sensitive to high frequency parameters;
- too optimistic on low frequency (steady state) parameters;
- disturbed if residuals are auto correlated.

The Simulation or Output Error Method is based on deterministic models to find parameters by minimising the error between simulation and measurement over a whole test period. Some characteristics are:

- more sensitive to low frequency parameters;
- too optimistic confidence intervals if residuals (here simulation errors) are auto correlated.

Several software tools have been developed for system identification purposes: CTSM [27], LORD [28] or the SIT in the MATLAB environment [29] being the most common.

In general, when the mathematical model for describing a physical phenomenon is only based on physical laws, it is the case of a white-box modelling (or deductive approach). This approach to the problem requires only previous physical knowledge about the system. On the contrary, the black-box modelling (or inductive approach) is only based on statistics and no physical knowledge about the data and its nature are required. This, for instance, is the case of neural network models.

In between these two methods is the grey-box modelling approach, based on a combination of physical knowledge and statistics. By using these models, identification of the unknown parameters of the system and accurate simulation and prediction of the most influential variables are possible. Short- and long-time fluctuations of the heat transfer may be modeled, which raises the level of description of the dynamics provided by the model [30]. One advantage of grey-box models, as opposed to black box model, is the possibility to directly incorporate physical knowledge and other prior information. As opposed to white box models, parameter estimation in grey-box models tends to provide more reproducible results and less bias, because random effects due to process and measurement noise are not absorbed into the parameter estimates but specifically accounted for by the diffusion and measurement noise terms [31].

Stochastic grey-box modelling approach is a well proven and accurate method for the characterization of dynamic systems [32, 33, 34]. It has been used for the estimation of U- and g-values

of buildings and components and for the identification of dynamical properties and dominant time constants for a better integration of renewable energies in buildings. Several studies are reported in literature [33, 35, 34] and the theoretical basis of stochastic grey-box models are outlined in the Annex I.

Considering double skin BIPV applications, different authors developed identification models that fit the experimental data by identifying suitable values to the unknown physical parameters of the system. Jiménez et al. [33] developed several grey-box models for the energy transfer evaluation of a double skin BIPV façade based on experimental data from the TRE in Ispra. The temperature of the PV module was chosen as the state and the output variable and different linear and non-linear models were presented. It was found that a non-linear single-state model was the most suitable for describing the dynamics convective and radiative of the BIPV energy balance. In [30], the model formulated in [33] was applied with different experimental data from the TRE, where transversal fins were placed in the air gap. Within this work, an exponential relation between the wind speed and the ambient convective coefficient was correctly identified for the specific set-up. The model described the experimental data satisfactory, but the authors suggested that an extension of the model from single-state to multiple-state might improve the performance of the model.

Results from evaluation work can be an input for model validation work. Modelling work intends to predict output data from validated models with identified or assumed parameters. Different authors developed numerical models of double skin BIPV systems [36, 37, 38, 39] using experimental data from double skin BIPV applications and an overview of the most important results is presented in Chapter 2.

2. Objectives and structure of the Thesis

2.1. Objectives and methodology

The general aim of this work is to contribute to the energy dynamic characterization of mechanically ventilated double skin BIPV systems under real outdoor conditions. In order to meet the general aim, a set of specific objectives were established. Starting from the analysis of the state of the art, one of the objectives of the present work was to experimentally investigate the energy dynamic of mechanically ventilated double skin BIPV systems by collecting reliable experimental data under outdoor conditions by means of an outdoor test facility. The aim was to provide reliable experimental data of ventilated double skin BIPV systems under different configurations, evaluating the effect of the ventilation airflow rate, the inclination and the rear-facing surface over the energy performance of the system. Another specific objective of the Thesis was to obtain the correct identification of the unknown physical parameters which take part in the energy balance, i.e. the heat transfer coefficients within the air gap and the PV module heat capacity, by using continuous-discrete stochastic state space grey-box models. After their correct identification, the models had to be statistically validated with several set of data from the experimental work, evaluating their uncertainty, upon which further development can be based. In addition, from the experience achieved during the experimental, analysis and modelling work, the final goal was the definition of a standardized set-up for testing double skin applications of BIPV under real outdoor conditions.

2.2. Structure of the Thesis

To meet the objectives outlined, the work has been organized in 4 interrelated specific stages which link with the following 4 Chapters of the Thesis. The Thesis is structured as a collection of papers, published in international peer-reviewed journals or to be submitted for publication. The remaining of the work is therefore organized as follows:

Chapter 2: The first paper of the Thesis presents the state of the art of double skin BIPV systems. In this article, a comprehensive review on existing testing, analysis and modelling work on ventilated BIPV systems is presented. Mechanically driven air flow rates are considered in the cavity, and the category of ventilated semi-transparent BIPV applications is highlighted.

Chapter 3: Since the analysis of the state of the art shows that only few data are currently available on the actual performances of these systems under real outdoor conditions and on the influence of different design parameters, the second stage has consisted in collecting experimental data by means of an outdoor test facility. From the experience gained in several research projects and the collaboration with the EC JRC research center in Ispra (Italy), an improved version of the Test Reference Environment (TRE) has been designed and constructed at the Lleida Agri-food Science and Technology Park (PCiTal). The paper describes the design and the measurement set-up of the TRE in Lleida and the extensive monitoring campaign carried out over a one year period. Several experiments, at different inclinations and ventilation regimes, have been performed. The influence of two different rear-facing materials has been also investigated. The electrical production

and the temperature of the ventilated PV panel placed at the TRE have been compared with the performance of two other identical PV modules which represent, respectively, the worst and the best condition: one reference module is fully insulated and the other one is left under free-rack conditions. Sensitivity analysis of the experimental results for a glass-tedlar PV module has been presented.

Chapter 4: This follows a third paper that presents the developed continuous-discrete stochastic grey-box models for the energy transfer assessment of the tested double skin BIPV system. The developed grey-box models enable identification of unknown parameters in the system and accurate prediction of the most influential variables. In the article, both one-state and two-state non-linear grey-box models are considered and the software implementation is described. In order to validate the results, the residuals are analysed for white-noise properties. The models are evaluated in time and frequency domain and the estimated Nusselt numbers are compared with values from literature relations. This paper was prepared in collaboration with the IMM Department of the Technical University of Denmark, where the candidate spent her six-month temporary stay.

Chapter 5: Finally, the last article included in this work is the proposal for a standard outdoor Test Reference Environment for double skin BIPV systems. This paper was prepared in collaboration with the European Commission DG JRC of Ispra, Italy. The proposal originated from the experience gained during the last ten years based on the experimental, analysis and modelling work carried out at the TRE in Ispra and Lleida.

The Thesis concludes with a general discussion of the results and the conclusions. The publication status of the papers is also included.

Complementary, as additional information to improve the understanding of the whole Thesis, the mathematical basis of the developed stochastic grey-box models have been included. They have been considered fundamental to complete this document because they describe several concepts used in the present work, especially in Chapter 4. A complete outline can be found in [40].

References

[1] (97)-599-COM, "Final energy for the future - renewable sources of energy: white paper," 1997.

[2] "Kyoto protocol. united nations framework convention on climate change." http://www.unfccc.int, Nov. 2009.

[3] "Directive 2009/28/EC of the european parliament and of the council of 23 april 2009 on the promotion of the use of energy from renewable sources and amending and subsequently repealing directives 2001/77/EC and 2003/30/EC," pp. 16–62, Official Journal of the European Union, L140, 2009.

[4] E. Parliament, "Directive 2002/91/EC of the european parliament and of the council of 16 december 2002 on the energy performance of buildings," 2002.

[5] E. Parliament, "Directive 2010/31/EU of the european parliament and of the council of 19 may 2010 on the energy performance of buildings," 2010.

[6] E. Standard, "EN 13779:2007. ventilation for non-residential buildings - performance requirements for ventilation and room-conditioning systems," 2007.

[7] J. Bloem and P. Baker, "Building integration issues for photovoltaics," in *Proceedings of BIAT - Technical Innovation in Design and Contruction*, (Dublin Castle), 2000.

[8] BBRI, "Source book for a better understanding of conceptual and operational aspects of active facades," 2002.

[9] A. Zollner, E. Winter, and R. Viskanta, "Experimental studies of combined heat transfer in turbulent mixed convection fluid flows in double-skin-facades," *International Journal of Heat and Mass Transfer*, vol. 45, pp. 4401–4408, 2002.

[10] D. Saelens, *Energy Performance Assessment of Single Storey MultipleSkin Facades.* Ph.D. thesis, Katholieke Universiteit Leuven, Leuven, Belgium, 2002.

[11] V. Serra, F. Zanghirella, and M. Perino, "Experimental evaluation of a climate facade: Energy efficiency and thermal comfort performance," *Energy and Buildings*, vol. 42, pp. 50–62, 2010.

[12] P. Wouters, L. Vandaele, P. Voit, and N. Fisch, "The use of outdoor test cells for thermal and solar building research within the PASSYS project," *Building and Environment*, vol. 28, pp. 107–113, 1993.

[13] D. van Dijk and R. Versluis, "PV-HYBRID-PAS: results of thermal performance assessment," in *Proceedings of the 2nd World Conference on Photovoltaic Solar Energy Conversion*, (Vienna), 1998.

[14] J. Jol, J. Bloem, B. Cross, M. Sandberg, K. Wambach, W. Wiesner, R. van Zolingen, and M. van Schalkwijk, "Towards a CE mark for PV building integrated systems," in *Proceedings of the 16th European Photovoltaic Solar Energy Conference*, (Glasgow), 2000.

[15] M. Sandberg and B. Moshfegh, "Buoyancy-induced air flow in photovoltaic facades effect of geometry of the air gap and location of solar cell modules," *Building and Environment*, vol. 37, pp. 211–218, 2002.

[16] T. Fung and H. Yang, "Study on thermal performance of semi-transparent building-integrated photovoltaic glazings," *Energy and Buildings*, vol. 40, pp. 341–350, 2008.

[17] A. Lloret, O. Aceves, L. Sabata, J. Andreu, J. Merten, M. Chantant, and U. Eicker, "Lessons learned in the electrical system design, installation and operation of the mataro public library," in *Proceeding of 14th European Photovoltaic Solar Energy Conference*, (Barcelona), 1997.

[18] S. Jensen, "Results from measurements on the PV-VENT systems at lundebjerg," Tech. Rep. Report SEC-R-14, Danish Technological Institute, Energy Division, 2001.

[19] E. Bakker, "Ecobuild research: full-scale testing of innovative technologies for energy efficient houses," 2004.

[20] D. Infield, "Design, study and experimental evaluation of an integrated solar facade.," tech. rep., 2000.

[21] G. Flamant, X. Loncour, and P. Wouters, "Performance assessment of active facades in outdoor test cells," in *EPIC 2002 AIVC Conference*, (Lyon, France), 2002.

[22] J. Bates, U. Blieske, J. Bloem, J. Campbell, F. Ferrazza, R. Hacker, P. Strachan, and Y. Tripanagnostopoulos, "Building implementation of photovoltaics with active control of temperature," in *Proceedings of the 17th European Photovoltaic Solar Energy Conference*, (Munich), 2001.

[23] J. Bloem, "Evaluation of a PV-integrated building application in a well-controlled outdoor test environment," *Building and Environment*, vol. 43, pp. 205–216, 2008.

[24] J. Bloem, "The JRC PV reference module for an energy rate indicator," in *Proceedings of the 16th European Photovoltaic Solar Energy Conference*, (Glasgow), 2000.

[25] J. Bloem, *System identification applied to building performance data.* Joint Research Centre, European Commission, 1994.

[26] INIVE-EEIG, *Stimulating increased energy efficiency and better building ventilation.* 2010.

[27] N. Kristensen and H. Madsen, *Continuous Time Stochastic Modelling - CTSM 2.3 - Mathematics Guide.* 2003.

[28] O. Gutschker, "Logical r determination (LORD) - modelling and identification software for thermal systems, user manual," 2004.

[29] "MATLAB - high performance numeric computation and visualization software. reference guide.," 1992.

[30] N. Friling, *Stochastic modelling of building integrated photovoltaic modules.* Master's thesis, Informatics and mathematical modelling, Technical University of Denmark, 2006.

[31] N. Kristensen, H. Madsen, and S. Jorgensen, "Parameter estimation in stochastic grey-box models," *Automatica*, vol. 40, pp. 225–237, 2004.

[32] H. Madsen and J. Holst, "Estimation of continuous-time models for the heat dynamics of a building," *Energy and Buildings*, vol. 22, pp. 67–79, 1995.

[33] M. Jimenez, H. Madsen, J. Bloem, and B. Dammann, "Estimation of non-linear continuous time models for the heat exchange dynamics of building integrated photovoltaic modules," *Energy and Buildings*, vol. 40, pp. 157–167, 2008.

[34] P. Bacher and H. Madsen, "Identifying suitable models for the heat dynamics of buildings," *Energy and Buildings*, vol. 43, pp. 1511–1522, 2011.

[35] N. Friling, M. Jimenez, J. Bloem, and H. Madsen, "Modelling the heat dynamics of building integrated and ventilated photovoltaic modules," *Energy and Buildings*, vol. 41, pp. 1051–1057, 2009.

[36] F. Christ, "Comparison of measured and predicted data for PV hybrid systems," 2001.

[37] A. Gandini, "Analisi numerica delle facciate fotovoltaiche a "doppia pelle"," 2002.

[38] J. Cipriano, C. Lodi, D. Chemisana, G. Houzeaux, and H. Perpinan, "Development and characterization of semitransparent double skin PV facades," in *Proceedings of the 1st International Conference on Solar Heating, Cooling and Buildings*, (Lisbon), 2008.

[39] L. Mei, D. Infield, U. Eicker, and V. Fux, "Thermal modelling of a building with an integrated ventilated PV faÃ§ade," *Energy and Buildings*, vol. 35, pp. 605–617, 2003.

[40] H. Madsen, *Time series analysis*. New York: Chapman and Hall/CRC, 2008.

Chapter 2: State of the art

C. Lodi, J. Cipriano, D. Chemisana, J.I. Rosell, State of the art on double skin BIPV systems: testing, analysis and modelling work, to be submitted for publication

Lodi C, Cipriano J, Chemisana D, Rosell J.I. State of the art on double skin BIPV systems: testing, analysis and modelling work. Submitted.

Chapter 3: Experimental work

C. Lodi, J. Cipriano, D. Chemisana, J.I. Rosell, Experimental evaluation of the overall energy performance of a mechanically ventilated double skin BIPV component in a controlled Test Reference Environment, to be submitted for publication

Lodi C, Cipriano J, Chemisana D, Rosell J.I. Experimental evaluation of the overall energy performance of a mechanically ventilated double skin BIPV component in a controlled Test Reference Environment. Submitted.

Chapter 4: Modelling work

C. Lodi, P. Bacher, J. Cipriano, H. Madsen, Modelling the heat dynamics of a monitored Test Reference Environment for Building Integrated Photovoltaic systems using stochastic differential equations, Energy and Buildings, In Press, Accepted Manuscript

Energy and Buildings xxx (2012) xxx–xxx

Contents lists available at SciVerse ScienceDirect

Energy and Buildings

journal homepage: www.elsevier.com/locate/enbuild

Modelling the heat dynamics of a monitored Test Reference Environment for Building Integrated Photovoltaic systems using stochastic differential equations

C. Lodi [a,*], P. Bacher [b], J. Cipriano [c], H. Madsen [b]

[a] Applied Physics Section of the Environment Science Department, University of Lleida, c/Jaume II 69, 25001 Lleida, Spain
[b] IMM, Technical University of Denmark, Richard Pedersen Plads, Building 305, 2800 Lyngby, Denmark
[c] CIMNE, Building Energy and Environment Group, c/Dr Ulles 2, 08224 Terrassa, Spain

ARTICLE INFO

Article history:
Received 14 January 2012
Received in revised form 8 March 2012
Accepted 25 March 2012

Keywords:
BIPV systems
Forced convection
Grey-box modelling
Parameter identification

ABSTRACT

This paper deals with grey-box modelling of the energy transfer of a double skin Building Integrated Photovoltaic (BIPV) system. Grey-box models are based on a combination of prior physical knowledge and statistics, which enable identification of the unknown parameters in the system and accurate prediction of the most influential variables. The experimental data originates from tests carried out with an air-based BIPV system installed in a Test Reference Environment. BIPV systems represent an interesting application for achieving the requirements of the EU EPBD Directive. Indeed, these systems could reduce the ventilation thermal losses of the building by pre-heating the fresh air. Furthermore, by decreasing PV module temperature, the ventilation air heat extraction can simultaneously increase electrical and thermal energy production of the building. A correct prediction of the PV module temperature and heat transfer coefficients is fundamental in order to improve the thermo-electrical production.

The considered grey-box models are composed of a set of continuous time stochastic differential equations, holding the physical description of the system, combined with a set of discrete time measurement equations, which represent the data driven part.

In the present work, both one-state and two-state non-linear grey-box models are considered. In order to validate the results, the residuals are analysed for white-noise properties.

1. Introduction

The aim of the present work is to carry out an energy transfer characterization of an air-based double skin Building Integrated Photovoltaic (BIPV) system. One of the encompassing results of this work is to model the effect of the PV module temperature in order to optimize BIPV installations under forced convection where the ventilation air is used for pre-heating the incoming air. The implementation of the EU EPBD Directive and the prEN 13779 has fixed considerable air renovations per hour for non-residential buildings, which results in an inevitable increase in the energy consumption, especially during the winter season. One possibility to reduce these ventilation thermal losses is the installation of BIPV systems in which the fresh air is pre-heated. These systems can thus substitute or be combined with the heat recovery unit of the building to take advantage of the waste heat. Since mechanical ventilation systems are normally installed in non-residential buildings, forced ventilation regimes are analysed in this work.

Reliable and detailed experimental data of air-based BIPV systems should be available for modelling purposes. During the PV-Hybrid-PAS EU project [1] a standard scheme for the performance evaluation of hybrid PV building components was developed. Within the IMPACT EU project [2] a common outdoor Test Reference Environment (TRE) [3] has been developed by the EU Joint Research Centre (JRC) in Ispra in order to assess the thermal exchange of the PV module with its environment. TRE is a standard outdoor facility for testing building integrated PV ventilated modules under forced regimes. With the experience gained from TRE experimental work, an improved version (Test Reference Environment of Lleida (TRE-L) as shown in Fig. 1) [4] was designed and built in the Lleida Outdoor Test centre (LOTCE). Several experiments, at different inclinations and ventilation regimes, have been performed and the initial experimental results are reported in [5]. Since TRE-L test facility is well insulated behind and on the lateral sides of the air channel, the effect of different rear-facing materials over the system can also be evaluated.

Different authors [6–8] have modelled the energy transfer of BIPV systems with continuous-discrete stochastic state space models based on experimental data. Grey-box modelling, based on stochastic differential equations (SDE's), is a well proven and promising method for describing the heat dynamics of buildings

* corresponding author. Tel.: +34 973003574.
E-mail addresses: chiara.lodi@macs.udl.cat (C. Lodi), pb@imm.dtu.dk (P. Bacher), cipriano@cimne.upc.edu (J. Cipriano), hm@imm.dtu.dk (H. Madsen).

0378-7788/$ – see front matter © 2012 Elsevier B.V. All rights reserved.
http://dx.doi.org/10.1016/j.enbuild.2012.03.046

Nomenclature

A	area [m^2]
c_p	specific heat coefficient at constant pressure [J/kgK]
C	heat capacity [J/K]
D_h	hydraulic diameter [m]
F	view factor of the PV module surface [–]
G	solar irradiance [W/m^2]
hc	convective heat transfer coefficient [W/m^2K]
IAM	incidence angle modifier [–]
k	thermal conductivity [W/mK]
$\dot{m}$	air mass flow rate [m^3/s]
Nu	Nusselt number [–]
q_e	specific electricity production [W/m^2]
Q_{abs}	absorbed heat flow [W]
Qc	convective heat flow rate [W]
Qe	electricity production [W]
Qr	radiative heat flow rate [W]
t	time [s]
T	temperature [K]
v	velocity [m/s]

Greek symbols

α	absorptance [–]
ΔT	air temperature difference between outlet and inlet air [K]
ϵ	longwave emissivity [–]
η	efficiency [–]
ϕ	tilt angle of the surface [°]
ρ	density [kg/m^3]
σ	Stefan–Boltzmann constant [W/m^2K^4]
τ	transmittance [–]
θ_{aoi}	angle of incidence [°]

Subscripts

amb	ambient
back	rear-facing material
bot	bottom
cells	PV cells
dew	dew point
gap	air gap
gl	glass
gnd	ground
in	inlet
m	measured
n	normal
out	outlet
PV	photovoltaic module
t	total
ted	tedlar
tr	transparent part of the PV module
w	wind

and components [9]. These dynamic models allow parameter estimation (system identification) and accurate prediction of the most influential variables. Grey-box models are composed by a set of stochastic differential equations, combined with a set of discrete time measurement equations. The SDE's hold the physical description of the system while the measurement equations represent the data driven part. One of the advantages of these models is the possibility to decompose the system noise into process noise and measurement noise. This allows for estimation of the unknown parameters in a *prediction error* (PE) setting as opposed to the common *output error* (OE) setting [6]. The models can be used for simulation, prediction and control applications.

Previous grey-box modelling work with TRE data from JRC was carried out by Jiménez et al. [6]. Within this work a non-linear model was found to be most suitable to describe the system and the authors emphasized that it was not possible to directly estimate the unknown physical parameters without more detailed measurements. In [7] the model formulated in [6] was applied with different experimental data from TRE prototype where transversal fins were placed in the air gap. The model described the experimental data satisfactory, but the authors suggested that an extension of the model from single-state to multiple-state might improve the performance of the model.

The grey-box models proposed in the present paper can be considered as an extension to the models described in [6,7]; the most relevant differences with the previous work is the direct estimation of the convective heat transfer coefficients between the PV module and the air gap, and the PV module heat capacity described through a single and a two-state model formulations. In addition, other physical inputs and outputs are also considered in the presented models: the angular dependency of the optical properties of the PV module, the electricity production, the effect of PV module inclination over the heat transfer coefficients and the consideration of the ground and sky temperatures for the radiative losses calculations. The estimated convective heat transfer coefficients within the air gap are also compared with the coefficients calculated from [10–14].

The paper starts with a description of the experimental set-up and data. Then follows a section about the modelling approach where the grey-box models structure and the considered models are presented. The following section summarizes the results of the modelling work: starting with a description of the estimated parameters, followed by the model evaluation in time and frequency domain and followed by a comparison of the estimated Nusselt numbers with literature relations. Finally conclusions are drawn and further developments are outlined.

2. Experimental set-up

2.1. Description of the set-up

The TRE-L prototype (see Fig. 1) is composed by a thermally well insulated wooden box (with external sizes of $2.06 \times 2.36 \times 0.37$ m) and a support structure which allows any inclination to be tested. The wooden box is filled with a 0.2 m thick expanded polystyrene (EPS) layer and the walls are formed by 0.02 m thick plywood painted with white varnish to minimize solar absorption. The prototype has a south facing opening where a glass-tedlar monocrystalline-Si PV module (with dimensions of 0.976×1.507 m) is positioned. The air channel behind the PV module is 0.115 m wide and its cross sectional area is 0.112 m^2. The hydraulic diameter is 0.198 m. The air enters from the bottom and is extracted from the top by means of a 0.125 m diameter PVC tube, placed at the rear side of the box so that it remains shaded. A variable speed fan controls the airflow at several rates. An array of plastic made cylindrical tubes with a diameter of 0.005 m is placed at the inlet to guarantee a non disturbed pattern flow. The PV module can easily be removed in order to access the rear side of the air gap. This allows different rear-facing materials to be tested. In the experiments used for this analysis an ALANOD-Mirotherm absorber sheet was positioned. This Mirotherm absorber is black coloured and it has a solar absorption of 90 ± 1 % (in the range of wavelength between 380 and 1650 nm) and a thermal emission of 5 ± 2 % (in the range of wavelength between 3 and 20 μm). The PV module is formed by 28 monocrystalline-Si solar cells (46 % area covered by

Please cite this article in press as: C. Lodi, et al., Modelling the heat dynamics of a monitored Test Reference Environment for Building Integrated Photovoltaic systems using stochastic differential equations, Energy Buildings (2012), http://dx.doi.org/10.1016/j.enbuild.2012.03.046

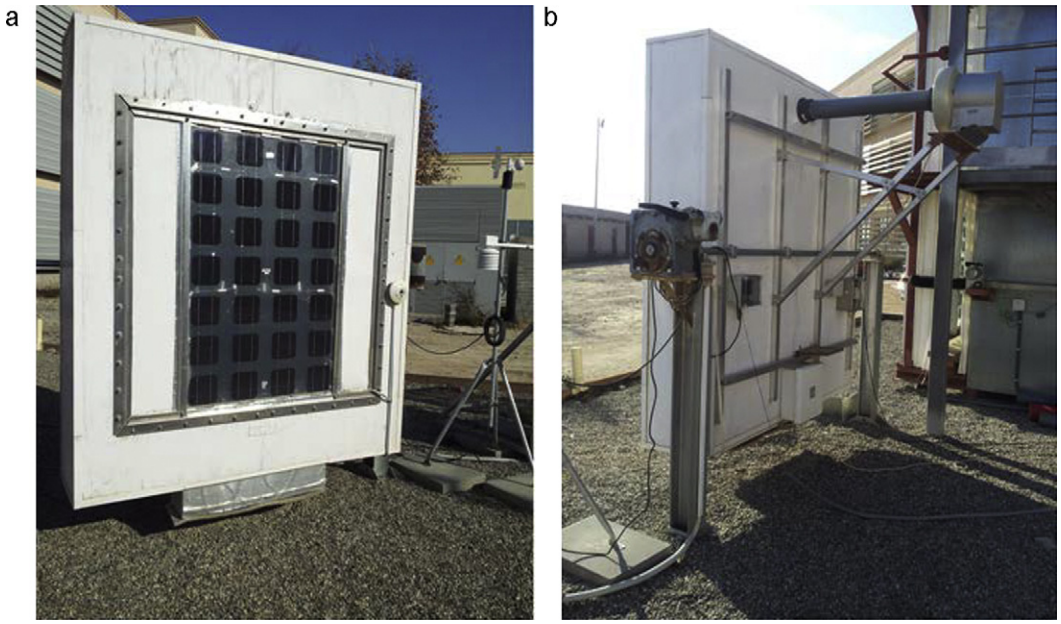

Fig. 1. Test Reference Environment of Lleida (TRE-L). (a) Front view; (b) rear view.

PV cells). In Fig. 2 an outline of the TRE-L measurement set-up is shown.

2.2. Experimental data

The data was collected in 30 s intervals and then averaged to 10 min values. The overall measurement period covers July to December 2010 and the trials consisted of 2–4 day period tests. The following temperatures were measured: inlet and outlet temperatures within the air gap, surface temperature of the interior side of the PV module, and surface temperature of the black absorber sheet. The electrical energy production of each string of the PV module was recorded in the data logger. Wind direction and speed were recorded by a cup-type anemometer placed next to the TRE-L and at the same height; ambient temperature and humidity were collected by a weather station placed approximately 10 m above the ground. For a detailed description of the experimental set-up and sensors, see [5].

The monitoring campaign was extended over a half year period. Tests on the TRE-L prototype were carried out with a fixed air gap width of 11.5 cm, two different inclinations (vertical and 30°) and seven ventilation regimes. Experimental results from the first part of the monitoring campaign are summarized in [5]. Fig. 3 shows plots of measured PV module average temperature, air inlet and outlet temperatures, and solar radiation for different air flow rates in the air cavity. As demonstrated, both PV module and outlet air temperatures are strongly affected by variations in solar radiation. The dynamical response of both variables is delayed in time because of the system thermal inertia. This indicates that a description of the dynamics when modelling on this time resolution is essential.

3. Energy transfer

Fig. 4 shows the energy transfer processes which occur when the PV ventilated module is exposed to solar radiation. The model takes on adiabatic conditions behind and to the lateral sides of the air channel.

The following heat transfer processes are considered within the system:

- Radiative heat losses to the exterior:

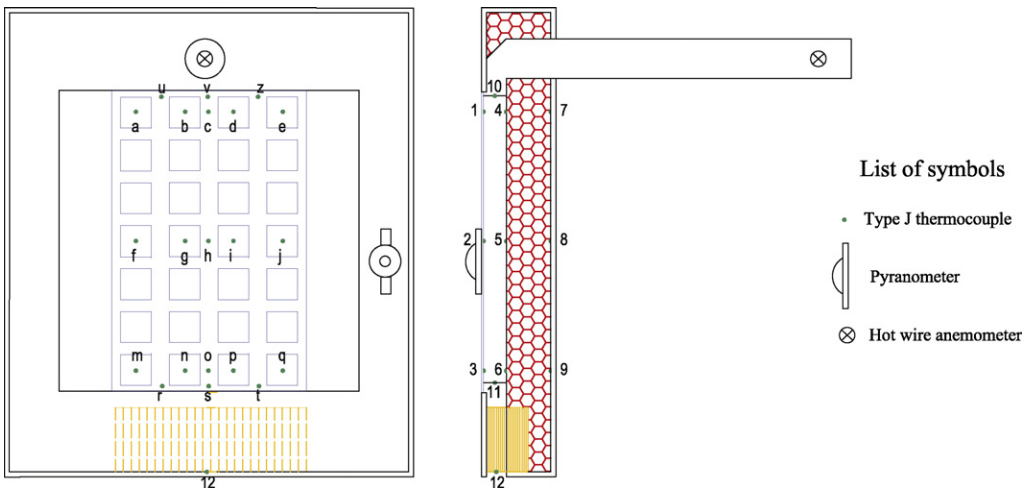

Fig. 2. Measurement set-up of the TRE-L prototype.

Please cite this article in press as: C. Lodi, et al., Modelling the heat dynamics of a monitored Test Reference Environment for Building Integrated Photovoltaic systems using stochastic differential equations, Energy Buildings (2012), http://dx.doi.org/10.1016/j.enbuild.2012.03.046

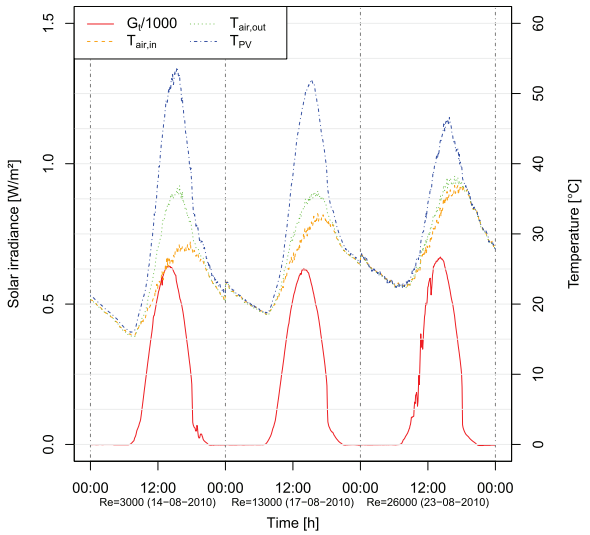

Fig. 3. Measured PV module average temperature, air inlet and outlet temperatures, and solar radiation for different air flow rates.

$$Qr_{PV,sky} = A_{PV}\,\sigma\,\epsilon_{gl}\,F_{sky}(T_{PV}^4 - T_{sky}^4) + A_{PV}\sigma\,\epsilon_{gl}\,F_{gnd}(T_{PV}^4 - T_{gnd}^4) \quad (1)$$

- Convective heat transfer between the PV module and the exterior:

$$Qc_{amb} = hc_{PV,amb}\,A_{PV}(T_{PV} - T_{amb}) \quad (2)$$

- Solar radiation absorbed by the PV module and electricity production:

$$Q_{abs} = A_{cells}(\tau\alpha)_{n,cells}G_t\,\mathrm{IAM}(\theta_{aoi}) + A_{tr}(\tau\alpha)_{n,tr}G_t\,\mathrm{IAM}(\theta_{aoi}) \quad (3)$$

$$Q_e = A_{PV}\,q_e \quad (4)$$

- Thermal radiative heat transfer between the PV module and the rear-facing material:

$$Qr_{PV,back} = \frac{A_{PV}\sigma}{(1/\varepsilon_{ted}) + (1/\varepsilon_{back}) - 1}(T_{PV}^4 - T_{back}^4) \quad (5)$$

- Convective heat transfer within the air channel:

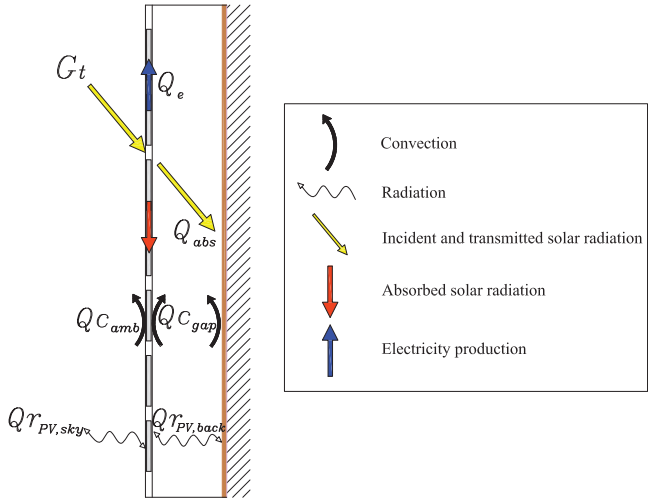

Fig. 4. Heat transfer processes within the TRE-L prototype.

$$Qc_{gap} = hc_{PV,gap}\,A_{PV}(T_{PV} - T_{gap}) + hc_{back,gap}\,A_{PV}(T_{back} - T_{gap}) = \dot{m}\rho_{gap}c_p\triangle T \quad (6)$$

These heat transfer processes are considered within the proposed models in Section 4.4.

4. Modelling approach

4.1. Model structure

The grey-box models are continuous time stochastic state space models, which are lumped capacitance models with addition of noise. The evolution in time of the lumped states is described by a set of continuous time stochastic differential equations (SDE's) (system equations):

$$dx_t = f(x_t, u_t, t, \theta)dt + \sigma(u_t, t, \theta)d\omega_t \quad (7)$$

which are indirectly observed as described by the set of discrete time measurement equations (measurement equations):

$$y_k = h(x_k, u_k, t_k, \theta) + e_k \quad (8)$$

where $x_t \in \chi \subset \mathbb{R}^n$ is a vector of state variables, $u_t \in \mathcal{U} \subset \mathbb{R}^m$ is a vector of input variables, $t \in \mathbb{R}$ is the time variable, $\theta \in \Theta \subset \mathbb{R}^p$ is a vector of parameters, $y_k \in \mathcal{Y} \subset \mathbb{R}^l$ is a vector of output variables. $f(\cdot) \in \mathbb{R}^n$, $\sigma(\cdot) \in \mathbb{R}^{nxn}$ and $h(\cdot) \in \mathbb{R}^l$ are known but possibly non-linear functions; $\{\omega\}$ is an n-dimensional standard Wiener process. $\{e_k\}$ is an l-dimensional white noise process with $e_k \in N(0, S(u_k, t_k, \theta))$, and $\sigma(\cdot)$ is the gain of the increments of the Wiener process. Hence the total noise in the model is decomposed into a process noise term (ω_t) and a measurement noise term (e_k) and they are assumed to be mutually uncorrelated. This allows for estimation of unknown parameters from experimental data in a prediction error setting as opposed to the more commonly used output error setting [6]. The process noise accounts for: modelling approximations (description of the dynamics, etc.), unrecognized and unmodeled inputs (not considered variables which may affect the system, etc.), and noise in the input measurements. The measurement noise term accounts for noise and drift in the output measurements [15].

4.2. Parameter estimation

The solution to Eq. (7) is a Markov process and unknown parameters of the model in Eq. (7) and (8) can be estimated with e.g., maximum likelihood or maximum a posteriori estimation [16]. Since no prior information about the parameters is available, maximum likelihood (ML) estimation is applied in the present modelling work. ML estimation of the unknown parameters is carried out by finding the parameters θ that maximize the likelihood function given a sequence of measurements Y_0, Y_1, …, Y_{N-1}, Y_N. By introducing the notation:

$$y_N = [Y_0,\ Y_1,\ \ldots,\ Y_{N-1},\ Y_N] \quad (9)$$

the likelihood function is the joint probability density:

$$L(\theta; y_N) = \left(\prod_{k=1}^{N} p(Y_k \mid \mathfrak{y}_{k-1}, \theta)\right) p(Y_0 \mid \theta) \quad (10)$$

where $p(Y_k \mid \mathfrak{y}_{k-1}, \theta)$ is a conditional density denoting the probability of observing Y_k given the previous observations and the parameters θ. $p(Y_0 \mid \theta)$ is the probability distribution function (pdf) of the starting conditions.

Please cite this article in press as: C. Lodi, et al., Modelling the heat dynamics of a monitored Test Reference Environment for Building Integrated Photovoltaic systems using stochastic differential equations, Energy Buildings (2012), http://dx.doi.org/10.1016/j.enbuild.2012.03.046

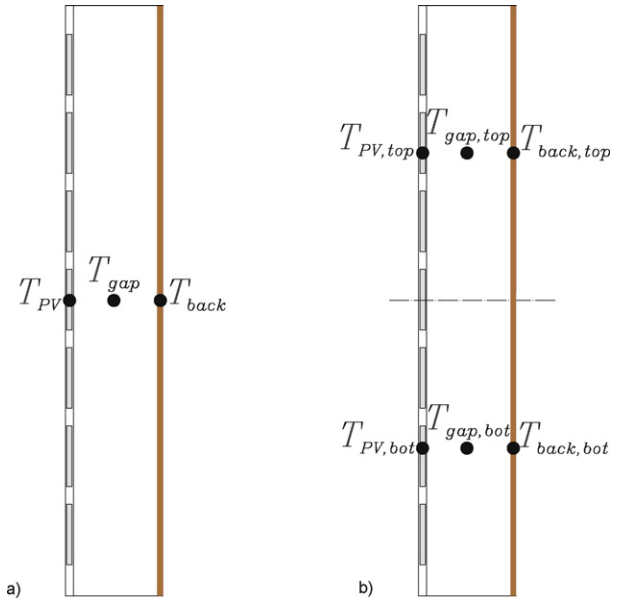

Fig. 5. Scheme of the estimation set-up. (a) Single-state model; (b) two-state model.

The maximum likelihood estimates of the parameters are then given by:

$$\hat{\theta} = arg\max_{\theta}\{L(\theta, y_N)\} \tag{11}$$

The covariance matrix is obtained by approximating the Fisher Information matrix with the inverse of the observed Hessian matrix evaluated at the final estimates. The uncertainties of the parameter estimates are obtained by decomposing the covariance matrix into a diagonal matrix of the standard deviations of the parameter estimates and the corresponding correlation matrix [17].

4.3. Software implementation

The parameter estimation described in Section 4.2 has been carried out using the software Continuous Time Stochastic Modelling CTSM [18]. CTSM is based on continuous-discrete stochastic state space models as described by Eqs. (7) and (8) and the extended Kalman filter (EKF) algorithm [16] is applied to find maximum likelihood estimates of the parameters in the model.

4.4. Considered grey-box models

The presented grey-box models can be used for both simulation and forecasting of the PV module temperature, and for the direct estimation of the unknown physical parameters of the system. The PV module temperature is defined as both state and output variable of the models and it is assumed spatially uniform at any instant within each control volume (assumption of the lumped capacitance method [11]).

Prior research [6,7] has demonstrated that non-linear models are the most appropriate for describing the dynamics of the present system. Within the present work, non-linear single and two-state models are presented. In Fig. 5 a scheme of the estimation set-up for both models is shown.

4.4.1. Single-state model formulation

The considered single-state model predicts the average PV module temperature while estimating unknown parameters of the system. Since measurements of the output variable are required, the PV module temperature is obtained as the averaged temperatures of the transparent and opaque areas. The presented model allows for an estimation of unknown physical parameters of the system (i.e. $hc_{PV,gap}$ and C_{PV}) and for statistically evaluating the accuracy of the estimates.

The single-state model for describing the heat dynamics of the PV module temperature in the TRE-L prototype can be expressed by the overall energy balance on the PV module surface:

$$\begin{aligned} C_{PV}dT_{PV} = \big(&A_{PV}\,hc_{PV,amb}(T_{amb} - T_{PV}) + A_{PV}\,hc_{PV,gap}(T_{gap} - T_{PV}) \\ &+ \frac{A_{PV}\sigma}{(1/\varepsilon_{ted}) + (1/\varepsilon_{back}) - 1}(T_{back}^4 - T_{PV}^4) + A_{PV}\,\sigma\epsilon_{gl}F_{sky}(T_{sky}^4 - T_{PV}^4) \\ &+ A_{PV}\,\sigma\,\epsilon_{gl}\,F_{gnd}(T_{amb}^4 - T_{PV}^4) + A_{cells}(\tau\alpha)_{n,cells}G_t\,\mathrm{IAM}(\theta_{aoi}) \\ &+ A_{tr}(\tau\alpha)_{n,tr}G_t\,\mathrm{IAM}(\theta_{aoi}) - A_{PV}\,q_e\big)\,dt + \sigma_1 d\omega_1 \end{aligned} \tag{12}$$

$$T_{PV,m} = T_{PV} + e \tag{13}$$

where Eqs. (12) and (13) are the system and observation equations, respectively.

The model has 10 inputs (v_w, T_{amb}, T_{gap}, T_{back}, F_{sky}, T_{sky}, F_{gnd}, θ_{aoi}, G_t, q_e),

8 known parameters (A_{PV}, A_{cells}, A_{tr}, ϵ_{ted}, ϵ_{back}, ϵ_{gl}, $(\tau\alpha)_{n,cells}$, $(\tau\alpha)_{n,tr}$) and 3 unknown parameters (C_{PV}, $hc_{PV,gap}$, σ_1) which are estimated.

Several necessary inputs and parameters are calculated as follows:

- The PV module total area is the sum of the PV cells and the transparent areas:

$$A_{PV} = A_{cells} + A_{tr} \tag{14}$$

- The temperature of the PV module is calculated as the average of PV cells and tedlar temperatures:

$$T_{PV,m} = \frac{T_{cells}A_{cells} + T_{tr}A_{tr}}{A_{PV}} \tag{15}$$

- The air gap temperature is calculated as a linear function of the inlet and outlet temperatures [19,20]:

$$T_{gap} = 0.25\,T_{air,in} + 0.75\,T_{air,out} \tag{16}$$

  Eq. (16) has been validated with air gap temperature measurements at mid-height of the TRE-L air gap.
- Since data of wind direction and speed is available, Sharples [21] relations are used for the exterior heat transfer coefficient, averaged for respectively windward and leeward directions:

$$hc_{PV,amb} = 3.72 + 1.16\,v_w \tag{17}$$

$$hc_{PV,amb} = 1.8 + 1.93\,v_w \tag{18}$$

- For non-normal solar incidence, the incidence angle modifier $\mathrm{IAM}(\theta_{aoi})$ is obtained by the expressions of Barker and Norton [22] for PV modules with clear glass:

$$\begin{aligned} \mathrm{IAM}(\theta_{aoi}) = 1 - (&3.3\,10^{-3}\theta_{aoi} + 4.12\,10^{-4}\theta_{aoi}^2 + 1.6\,10^{-5}\theta_{aoi}^3 \\ &+ 2.6\,10^{-7}\theta_{aoi}^4) \end{aligned} \tag{19}$$

- The longwave view factors of the PV module surface to respectively sky and ground surface are calculated as follows [23]:

$$F_{sky} = 0.5\,(1 + \cos\phi) \tag{20}$$

$$F_{gnd} = 0.5\,(1 - \cos\phi) \tag{21}$$

- Since data of the dew point ambient temperature is available, the Duffie and Beckman relation [24] has been used for the sky temperature calculation:

$$T_{sky} = T_{amb}(0.711 + 0.0056\,T_{dew} + 0.000073\,T_{dew}^2 + 0.013\cos(\pi\,t_m/12)) \tag{22}$$

where t_m is the time from midnight in hours and the ground temperature T_{gnd} is assumed to be the same as the ambient temperature. In previous works ([6,7]) the effective sky temperature was considered a steady-state parameter to estimate.

4.4.2. Two-state model formulation

Since the PV module, black absorber and air gap temperatures are collected at three different heights (see Fig. 2) and considerable differences (up to 10 °C) are found between top and bottom PV module temperatures, the single-state model has been extended to a two states formulation in order to get a better prediction. The need of using a multiple state model for the system description was expressed also in [7]. With the two-state model, top and bottom PV module average temperatures are estimated separately, taking the temperature gradient over the vertical axis into account. The two-state model is formulated as follows:

$$\frac{C_{PV}}{2}dT_{PVbot} = \left(\frac{A_{PV}}{2}hc_{PV,amb}(T_{amb} - T_{PVbot}) + \frac{A_{PV}}{2}hc_{PV,gap}(T_{gap,bot} - T_{PVbot}) + \frac{A_{PV}}{2}\frac{\sigma}{(1/\varepsilon_{ted}) + (1/\varepsilon_{back}) - 1}(T_{back,bot}^4 - T_{PVbot}^4) + \frac{A_{PV}}{2}\sigma\varepsilon_{gl}F_{sky}(T_{sky}^4 - T_{PVbot}^4) + \frac{A_{PV}}{2}\sigma\varepsilon_{gl}F_{gnd}(T_{gnd}^4 - T_{PVbot}^4) + \frac{A_{cells}}{2}(\tau\alpha)_{n,cells}G_t\,IAM(\theta_{aoi}) + \frac{A_{tr}}{2}(\tau\alpha)_{n,tr}G_t\,IAM(\theta_{aoi}) - \frac{A_{PV}}{2}\frac{q_e}{2}\right)dt + \sigma_1 d\omega_1 \tag{23}$$

$$\frac{C_{PV}}{2}dT_{PVtop} = \left(\frac{A_{PV}}{2}hc_{PV,amb}(T_{amb} - T_{PVtop}) + \frac{A_{PV}}{2}hc_{PV,gap}(T_{gap,top} - T_{PVtop}) + \frac{A_{PV}}{2}\frac{\sigma}{(1/\varepsilon_{ted}) + (1/\varepsilon_{back}) - 1}(T_{back,top}^4 - T_{PVtop}^4) + \frac{A_{PV}}{2}\sigma\varepsilon_{gl}F_{sky}(T_{sky}^4 - T_{PVtop}^4) + \frac{A_{PV}}{2}\sigma\varepsilon_{gl}F_{gnd}(T_{gnd}^4 - T_{PVtop}^4) + \frac{A_{cells}}{2}(\tau\alpha)_{n,cells}G_t\,IAM(\theta_{aoi}) + \frac{A_{tr}}{2}(\tau\alpha)_{n,tr}G_t\,IAM(\theta_{aoi}) - \frac{A_{PV}}{2}\frac{q_e}{2}\right)dt + \sigma_2 d\omega_2 \tag{24}$$

$$T_{PVbot,m} = T_{PVbot} + e_1 \tag{25}$$

$$T_{PVtop,m} = T_{PVtop} + e_2 \tag{26}$$

The model needs 12 inputs (v_w, T_{amb}, $T_{gap,bot}$, $T_{gap,top}$, $T_{back,bot}$, $T_{back,top}$, F_{sky}, T_{sky}, F_{gnd}, θ_{aoi}, G_t, q_e), 8 known parameters (A_{PV}, A_{cells}, A_{tr}, ϵ_{ted}, ϵ_{back}, ϵ_{gl}, $(\tau\alpha)_{n,cells}$, $(\tau\alpha)_{n,tr}$) and 4 unknown parameters (C_{PV}, $hc_{PV,gap}$, σ_1, σ_2) which are estimated.

The same assumptions as for the presented single state model are assumed.

The air gap temperatures are calculated by (see Fig. 5):

$$T_{gap,bot} = 0.25\,T_{air,in} + 0.75\,T_{gap} \tag{27}$$

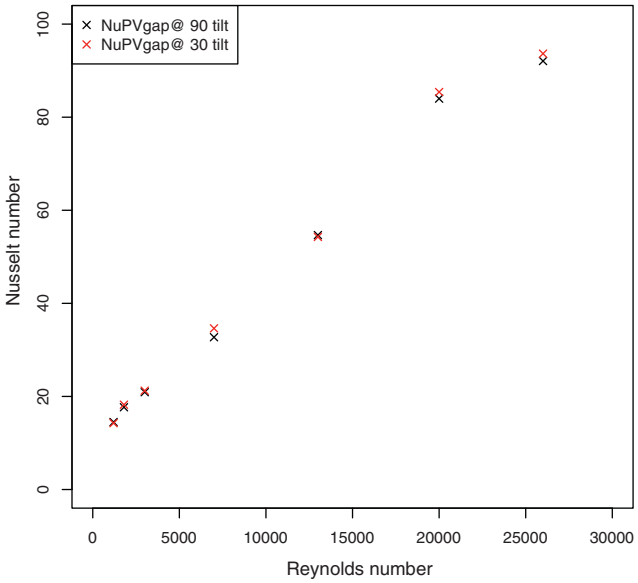

Fig. 6. Nusselt numbers for the PV module versus Reynolds numbers. Comparison of 90° and 30° tilt angles.

$$T_{gap,top} = 0.25\,T_{gap} + 0.75\,T_{air,out} \tag{28}$$

5. Results and discussion

5.1. Parameter estimation

In order to estimate the unknown parameters, partly clouded days are used for modelling. Using such days the heat transfer processes which are modelled are less correlated than for clear sky days, leading to a better parameter estimation. Once the parameters are estimated, sunny days are used to test the model.

The estimated parameters and the corresponding standard deviations are shown in Table 1.

As seen in Table 1, uncertainties on the parameters estimates decrease when passing from single to two-state model, confirming the necessity to take the temperature gradient over the vertical axis into account.

Starting the evaluation with the estimates of the convective heat transfer coefficients, the average Nusselt numbers are given by:

$$Nu_{PV,gap} = \frac{hc_{PV,gap}D_h}{k_{air}} \tag{29}$$

In Fig. 6, the estimated average Nusselt numbers are shown as a function of the Reynolds number (Re). The tests were performed in vertical position and at a 30° tilt angle and no significant differences are found for the Nusselt numbers. Similar results were found in [14].

Regarding the estimated values of C_{PV}, they differ slightly for distinct Reynolds numbers (see Table 1). Taking the uncertainties of the parameters estimate into account, the differences are however not statistically significant for Re >3000. For lower Reynolds numbers, the differences could be caused by non-modelled natural convection effects that could be included in more advanced models.

5.2. Model evaluation

5.2.1. Residuals analysis in time and frequency domain

In Fig. 7 plots of the residuals for the two-state model are shown. The residuals are plotted versus time, solar radiation, state variables and wind speed; these plots may reveal potential outliers or systematic dependencies of the residuals on inputs or states. It

Please cite this article in press as: C. Lodi, et al., Modelling the heat dynamics of a monitored Test Reference Environment for Building Integrated Photovoltaic systems using stochastic differential equations, Energy Buildings (2012), http://dx.doi.org/10.1016/j.enbuild.2012.03.046

Table 1
ML estimated parameters and the corresponding standard deviations in vertical position.

Model	Single-state model		Two-state model	
Ventilation regime	C_{PV}	$hc_{PV,gap}$	C_{PV}	$hc_{PV,gap}$
Re = 1200	20823 (± 1267)	1.56 (± 0.68)	16504 (± 281)	1.52 (± 0.19)
Re = 1800	–	–	16020 (± 151)	2.23 (± 0.08)
Re = 3000	18997 (± 519)	2.48 (± 0.08)	17958 (± 755)	2.52 (± 0.05)
Re = 7000	24262 (± 1698)	3.94 (± 0.13)	20788 (± 650)	4.77 (± 0.12)
Re = 13000	17735 (± 1615)	6.22 (± 0.25)	19088 (± 719)	6.85 (± 0.16)
Re = 20000	23056 (± 2043)	8.78 (± 0.30)	22180 (± 780)	10.78 (± 0.03)
Re = 26000	25924 (± 1153)	10.38 (± 0.21)	20278 (± 484)	11.62 (± 0.15)

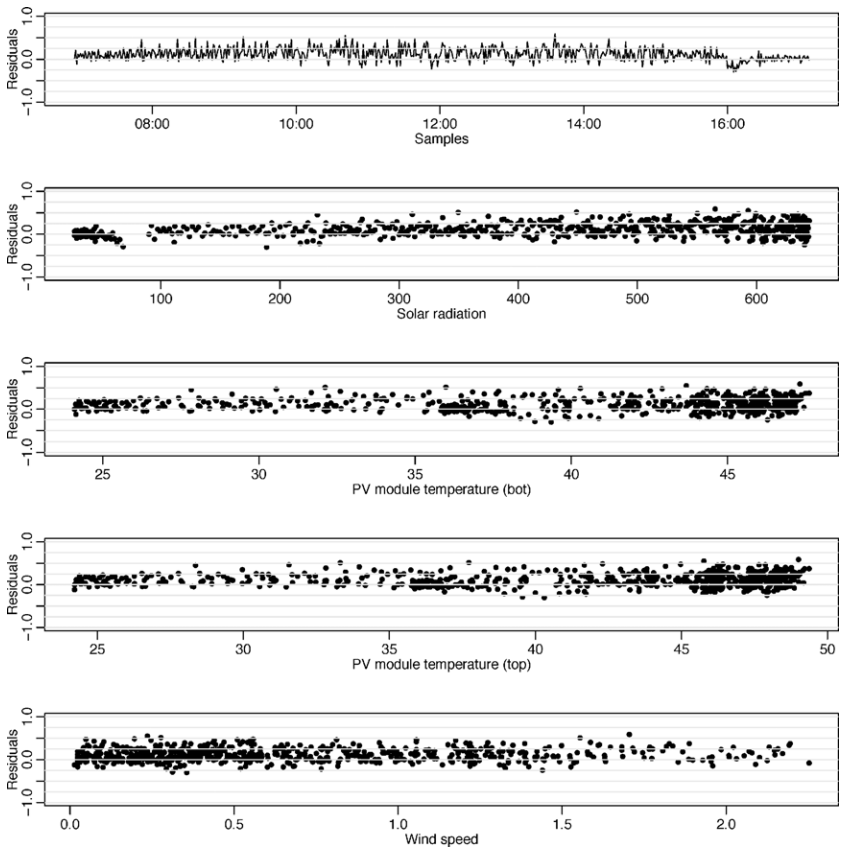

Fig. 7. Plots of the residuals of the two-state model for a one-day period (Re = 20000).

is possible to observe that the variance of the residuals increase slightly with solar radiation and PV module temperature, revealing that a possible model improvement could be the introduction of a dependency of these variables in the noise term of the model. A similar behavior is found also for the single-state model.

To verify that the model describes the dynamics of the system properly, the assumption of white noise residuals (one-step prediction) is checked. The white noise properties are analysed with the auto-correlation functions (ACF) and the cumulated periodograms (CP) plotted in Fig. 8. Confidence bands of approximately 95% under the hypothesis that the residuals are white noise are also shown. The ACF and the CP of the residuals clearly show that the two-state model describes the dynamics of the system better than the single-state model, and in fact it is concluded that a two state is needed to describe all the systematic variations in the data. For the two-state model the white noise assumption of the residuals is not rejected.

5.2.2. Simulation and prediction

As a further evaluation, the performance of the two-state model for both simulation and prediction is analysed. Fig. 9 shows simulated and measured T_{PVtop} for 1 min time step. A similar pattern is found for longer sample periods (i.e. 5 or 10 min). The simulated temperatures reasonably follow the observed temperature profile and the standard deviation of the temperature difference is (0.72 °C) for 1-min data and (0.75 °C) for 10 min data. The highest temperature differences are registered when there are fast changes in temperature. This is probably due to the fact that some fast dynamical effects are not adequately considered in the model and it reveals that in the simulation, long-time variations are better described than the short-time variations.

The one-step predictions of T_{PVtop} are compared with the observations in Fig. 10. A similar pattern is found for longer sample periods (i.e. 5 or 10 min). It is possible to observe that the model predicts accurately the PV module temperature and the standard deviation of the prediction error is (0.18 °C) for 1-min data and (0.6 °C) for 10 min data.

5.3. Comparison with literature relations for Nusselt numbers in forced convection

In order to compare the estimated Nusselt numbers with literature relations it is important to define weather the flow is

Please cite this article in press as: C. Lodi, et al., Modelling the heat dynamics of a monitored Test Reference Environment for Building Integrated Photovoltaic systems using stochastic differential equations, Energy Buildings (2012), http://dx.doi.org/10.1016/j.enbuild.2012.03.046

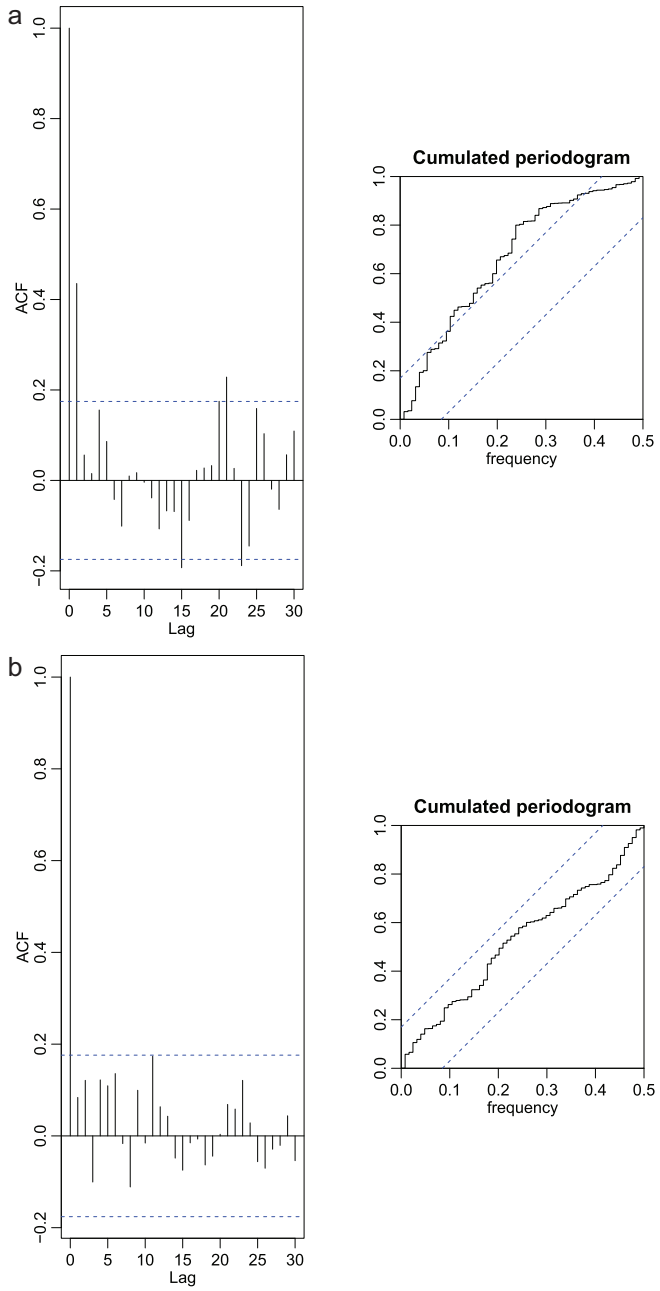

Fig. 8. The auto-correlation function and the cumulated periodogram of the residuals for the selected grey-box model. (a) Single-state model; (b) two-state model.

fully-developed or not. Therefore, the thermal entrance length (x_{th}) has been calculated with Bejan [25] relations. In both laminar and turbulent regimes, the fully developed heat transfer condition is not reached, since $x_{th} \approx 1.7\,m$ while the air gap length is 1.6 m.

In Fig. 11 the estimated Nusselt numbers are compared with values calculated from some of the most typical literature relations [10–14,26] for developing flow in channels with laminar, transient or turbulent regimes. There are only a few relations for developing flow in transient and turbulent regimes [11–13] because several authors [25,27] assume that in turbulent flow the entrance effects are not significant and that the flow is fully-developed for the entire channel length. Furthermore, literature relations are normally based on isothermal or isoflux boundary conditions but normally in a BIPV system neither isothermal nor isoflux boundary conditions are fulfilled. Relations for both symmetrical and asymmetrical heating are considered in Fig. 11 since the average

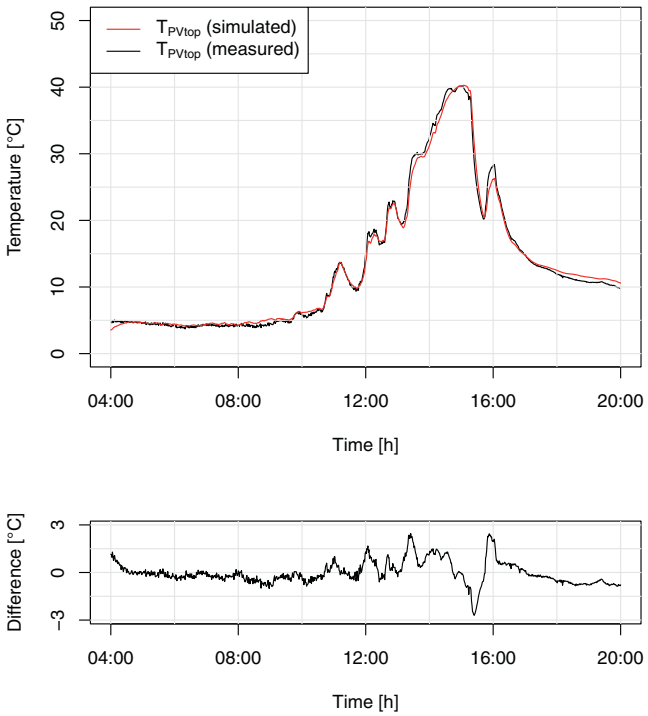

Fig. 9. Simulation and measurements of T_{PVtop} with the two-state model for 1 min data (Re = 1800; 07/01/2011).

temperature difference between the PV module and the black absorber is always lower than 4 °C. As it is possible to observe in Fig. 11, for the same Reynolds number, the Nusselt number value can be quite different when using different literature relations. Literature relations generally underestimate the identified Nusselt

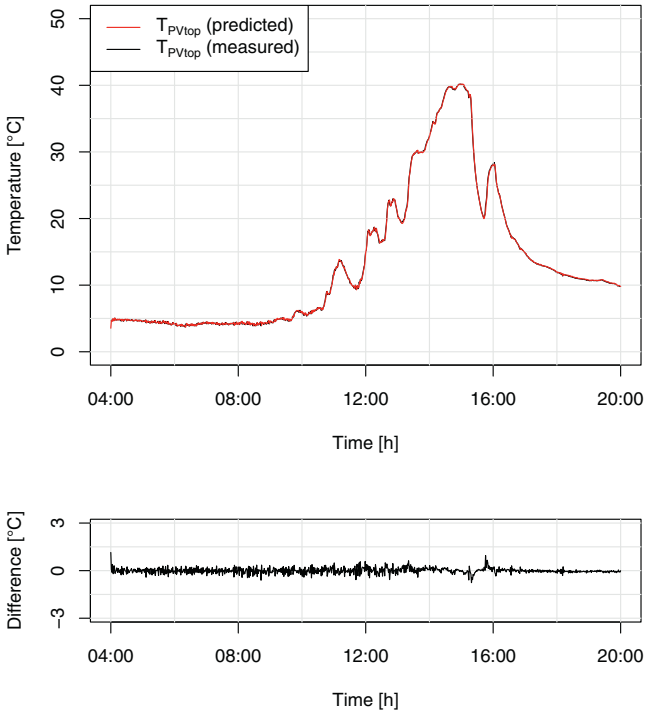

Fig. 10. One-step prediction and measurements of T_{PVtop} with the two-state model for 1 min data (Re = 1800; 07/01/2011).

Please cite this article in press as: C. Lodi, et al., Modelling the heat dynamics of a monitored Test Reference Environment for Building Integrated Photovoltaic systems using stochastic differential equations, Energy Buildings (2012), http://dx.doi.org/10.1016/j.enbuild.2012.03.046

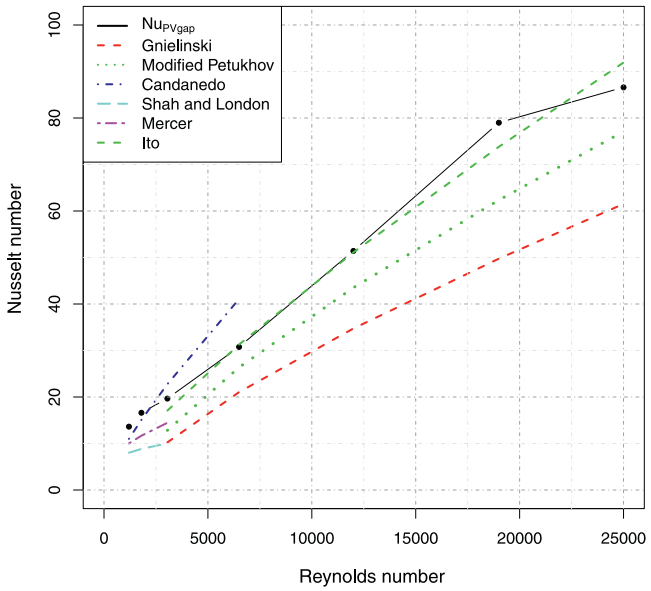

Fig. 11. Comparison of the estimated average Nusselt numbers with values from literature relations.

values. The result is in accordance with several studies on BIPV [3,14]. In this particular case, Ito relation [13] provides the best prediction of the estimated Nusselt numbers for transient and turbulent conditions ($R^2 = 0.985$). For Re <3000, Candanedo's relation predicts quite correctly the estimated values ($R^2 = 0.995$).

6. Conclusions and further developments

Continuous-discrete stochastic state space models are applied for modelling the heat dynamics of ventilated BIPV modules based on measured data from a well-controlled experimental set-up. The strength of grey-box models is the possibility to combine physical and data driven information in order to identify model parameters and providing information about uncertainties of the model. Within this study, both one-state and two-state grey-box models are presented, and it is shown that the two-state model provides the best description of the heat dynamics of the system and the two-state model is not contradicted by white noise tests. This reflects that the second model can be assumed to describe the information in the sampled measurements of the dynamics of the system.

The estimated parameters are evaluated both from a physical and a statistical point of view. Regarding the convective heat transfer coefficients between the PV module and the air gap, it is shown that the most typical literature relations predict quite different values for the same Reynolds number leading to possible calculation errors. In this particular case, the estimated values with the two-state model are predicted properly with the Ito's relation for transient and turbulent regimes, while in laminar conditions Candanedo's relation approximates quite accurately the estimated Nusselt numbers.

Regarding the estimated values of C_{PV}, they slightly differ for different Reynolds number, especially for lower Reynolds numbers; the differences are not statistically significant for Re >3000 and for lower values the difference could be caused by non-modelled natural convection effects that should be included in more advanced models.

The statistical evaluation of the two-state model shows that the model describes the dynamics of the system very well, and that a possible model improvement could be the introduction of a dependency of the solar radiation and the PV module temperature in the noise term.

One promising feature of grey-box models is also the possibility to be applied for simulation and prediction purposes. It is shown that the two-state model performs properly both in prediction and simulation context.

In order to check the reliability and to identify the most suitable model, likelihood ratio tests should be applied in future work [8].

Several rear-facing materials are planned to be tested in the TRE-L and the applicability of the presented models for different optical properties of the system should be verified in future work.

Acknowledgements

This work has been financially supported by a FPU program (ref. AP2008-01801) and ENE2010-18357 grants from the Spanish Ministry of Science and Innovation.

References

[1] D. van Dijk, R. Versluis, PV-HYBRID-PAS: results of thermal performance assessment, in: Proceedings of the 2nd World Conference on Photovoltaic Solar Energy Conversion, Vienna, 1998.
[2] J. Bates, U. Blieske, J. Bloem, J. Campbell, F. Ferrazza, R. Hacker, P. Strachan, Y. Tripanagnostopoulos, Building implementation of photovoltaics with active control of temperature, in: Proceedings of the 17th European Photovoltaic Solar Energy Conference, Munich, 2001.
[3] J. Bloem, Evaluation of a PV-integrated building application in a well-controlled outdoor test environment, Building and Environment 43 (2008) 205–216.
[4] J.J. Bloem, C. Lodi, J. Cipriano, D. Chemisana, An outdoor Test Reference Environment for double skin applications of Building Integrated PhotoVoltaic Systems, Energy and Buildings (2012), http://dx.doi.org/10.1016/j.enbuild.2012.03.023.
[5] C. Lodi, J. Cipriano, J. Bloem, D. Chemisana, Design and monitoring of an improved test reference environment for the evaluation of BIPV systems, in: Proceedings of the 25th European Photovoltaic Solar Energy Conference, Valencia, 2010, pp. 5135–5140.
[6] M. Jimenez, H. Madsen, J. Bloem, B. Dammann, Estimation of non-linear continuous time models for the heat exchange dynamics of building integrated photovoltaic modules, Energy and Buildings 40 (2008) 157–167.
[7] N. Friling, M. Jimenez, J. Bloem, H. Madsen, Modelling the heat dynamics of building integrated and ventilated photovoltaic modules, Energy and Buildings 41 (2009) 1051–1057.
[8] P. Bacher, H. Madsen, Identifying suitable models for the heat dynamics of buildings, Energy and Buildings 43 (2011) 1511–1522.
[9] H. Madsen, J. Holst, Estimation of continuous-time models for the heat dynamics of a building, Energy and Buildings 22 (1995) 67–79.
[10] R. Shah, A. London, Laminar flow forced convection in ducts, in: Advances in Heat Transfer, Academic Press, 1978.
[11] F. Incropera, D. De Witt, Fundamentals of Heat and Mass Transfer, John Wiley & Sons, New York, 1985.
[12] U. Eicker, Solar Technologies for Buildings, Wiley, Chichester, 2003.
[13] S. Ito, M. Kashima, N. Miura, Flow control and unsteady-state analysis on thermal performance of solar air collectors, Journal of Solar Energy Engineering 128 (2006) 354–359.
[14] L. Candanedo, A. Athienitis, K. Park, Convective heat transfer coefficients in a building-integrated photovoltaic/thermal system, Journal of Solar Energy Engineering ASME 133 (2011), pp. 021002-1-021002-14.
[15] H. Madsen, J. Holst, E. Lindstrom, Modelling non-linear and non-stationary time series, IMM,DTU (2007).
[16] H. Madsen, Time Series Analysis, Chapman and Hall/CRC, New York, 2008.
[17] H. Madsen, P. Thyregod, Introduction to General and Generalized Linear Models, CRC Press, 2010.
[18] N. Kristensen and H. Madsen, Continuous Time Stochastic Modelling – CTSM 2.3 – Mathematics Guide. 2003.
[19] J. Hirunrabh, W. Kongduang, P. Namprakai, J. Khendari, Study of natural ventilation of houses by a metallic solar wall under tropical climate, Renewable Energy 18 (1999) 109–119.
[20] K. Ong, A mathematical model of a solar chimney, Renewable Energy 28 (2003) 1047–1060.
[21] S. Sharples, Full-scale measurements of convective energy losses from exterior building surfaces, Building and Environment 19 (1984) 31–39.
[22] G. Barker, P. Norton, Building america system performance test practices: Part 1 – photovoltaic systems, NREL/TP-550-30301, National Renewable Energy Laboratory (NREL) (2003).
[23] G. Walton, Thermal Analysis Research Program Reference Manual, No. NBSSIR 83-2655 in National Bureau of Standards (1983).
[24] J.A. Duffie, W.A. Beckman, Solar Engineering of Thermal Processes, 3 ed., Wiley, 2006.
[25] A. Bejan, D. Kraus, Heat Transfer Handbook, John Wiley & Sons Ltd., 2003.
[26] H. Tan, M. Charters, An experimental investigation of forced convective heat transfer for fully-developed turbulent flow in a rectangular duct with asymmetric heating, Solar Energy 13 (1970) 121–125.
[27] L. Jiji, Heat Convection, Springer ed, 2006.

Please cite this article in press as: C. Lodi, et al., Modelling the heat dynamics of a monitored Test Reference Environment for Building Integrated Photovoltaic systems using stochastic differential equations, Energy Buildings (2012), http://dx.doi.org/10.1016/j.enbuild.2012.03.046

Chapter 5: Proposal for a standard TRE

J.J. Bloem, C. Lodi, J. Cipriano, D. Chemisana, An outdoor Test Reference Environment for double skin applications of Building Integrated Photovoltaic Systems, Energy and Buildings, In Press, Accepted Manuscript

Energy and Buildings xxx (2012) xxx–xxx

Contents lists available at SciVerse ScienceDirect

Energy and Buildings

journal homepage: www.elsevier.com/locate/enbuild

An outdoor Test Reference Environment for double skin applications of Building Integrated PhotoVoltaic Systems

J.J. Bloem [a], C. Lodi [b,*], J. Cipriano [c], D. Chemisana [b]

[a] European Commission DG JRC, via E. Fermi 2749, TP 450, 21027 Ispra (VA), Italy
[b] Applied Physics Section of the Environmental Science Department, University of Lleida, c/Jaume II 69, 25001 Lleida, Spain
[c] CIMNE, Building Energy and Environment Group, c/Dr Ulles 2, 08224 Terrassa, Spain

ARTICLE INFO

Article history:
Received 13 February 2012
Received in revised form 1 March 2012
Accepted 11 March 2012

Keywords:
Building Integrated PhotoVoltaic (BIPV) systems
Harmonisation
Outdoor testing
Dynamic analysis
Modelling

ABSTRACT

This article presents and discusses an outdoor Test Reference Environment (TRE) for double skin applications of Building Integrated PhotoVoltaic (BIPV) Systems.

From the experience gained during the past 20 years in several EC research projects, an experimental tested design for a common Test Reference Environment is proposed. This outdoor test set-up allows the assessment of experimental data for electrical and thermal performance evaluation of photovoltaic systems integrated as double skin applications in the building envelope. The specific design of the Test Reference Environment makes it possible to study in a harmonised way through electrical and thermal energy flow analysis, the impact of different materials for PV modules and construction design of building envelopes. The energy balance for BIPV double skin applications is presented as well.

The experimental data has been used for validation of modelling work by several academic groups which has resulted in an improved knowledge on the heat transfer, in particular the convective heat exchange coefficient for the specific double skin boundary conditions.

1. Introduction

Building Integrated PhotoVoltaic (BIPV) systems are building components that combine other functions of the building envelope with electricity generation. Double skin applications of BIPV systems appear as an attractive strategy for achieving the requirements of the new EU directive on energy performance of buildings (EPBD) [1], in particular the integration of renewable energy technologies supporting the design of nearly-zero energy buildings (NZEB). Double skin BIPV systems may improve the energy performance of the building envelope by decreasing the transmission losses in winter and by reducing solar gains in summer. Apart from generating electricity, the pre-heated air may reduce the ventilation thermal losses and therefore the heating demand of the building. At the same time, the pre-heated air might be coupled with a heating and ventilation air-conditioning (HVAC) system. Furthermore, the ventilation air heat extraction may decrease the PV module temperature, which will result simultaneously in an increase of PV electrical efficiency. In any case, a correct evaluation of the overall energy balance of these integrated systems is very complex due to highly variable and dynamic aspects.

Over the last 20 years, different EC projects have investigated the possibility to develop a standard outdoor environment for the energy performance evaluation of double skin applications of BIPV systems, giving input to modelling and analysis work.

Starting from the first EC PASSYS projects (1986–1994), it was found that BIPV system evaluation requires the combination of well-controlled experimental measurements under real climatic conditions with detailed simulation techniques. The EC PV-HYBRID-PAS project [2] (1994–1998) was aimed at developing standardised test procedures for the overall energy performance evaluation of hybrid PV building components. Tests on hybrid-PV components were carried out with both natural and forced ventilation using PASLINK test cells located in several different climates. Within this project an initial set-up of an outdoor Test Reference Environment (TRE) was outlined. One of the conclusions drawn from this project was that outdoor measurements of the energy balance must be performed under well-described and controlled conditions in order to use the data to calibrate numerical models. The PASLINK project [3] aimed to define quality requirements for outdoor testing and evaluation. Several partners in the PASLINK network carried out for industry experimental testing of PV intended for building integration.

The need for well-described and standardised testing conditions was the core issue of the EC PRESCRIPT project [4] (1997–1999) regarding the development and benchmarking of a pre-standard for testing PV roofs and facades. In the context of this European project

* Corresponding author.
E-mail addresses: cipriano@cimne.upc.edu (J. Cipriano), daniel.chemisana@udl.cat (D. Chemisana).

0378-7788/$ – see front matter © 2012 Elsevier B.V. All rights reserved.
doi:10.1016/j.enbuild.2012.03.023

Nomenclature

A	heat effective surface area [m^2]
c_p	specific heat coefficient of air [J/kgK]
G_t	total incoming solar radiation [W/m^2]
h_{cv}	convective heat exchange coefficient in the air gap [W/m^2K]
$\dot{m}$	air mass flow rate [kg/s]
N_i	distribution factor for the diffusely absorbed solar radiation [–]
Q_{abs}	absorbed heat flow [W]
Q_c	convective heat flow rate [W]
Q_e	electricity production [W]
Q_r	radiative heat flow rate [W]
R_{cv}	convective resistance of the PV module with the air in the air gap [m^2K/W]
R_{cv2}	convective resistance of the facing wall with the air in the air gap [m^2K/W]
R_e^*	thermal resistance between ambient and the air gap [m^2K/W]
R_i^*	thermal resistance between internal ambient and the air gap [m^2K/W]
R_{rd}	radiative resistance between the two air gap surfaces [m^2K/W]
T_{PV}	PV module average cell temperature [K]

Greek symbols

α_{est}	solar absorbance of the PV layer [–]
η	PV electrical efficiency (a function of cell temperature and solar irradiance) [–]
θ_f	inlet air temperature [K]
θ_{int}	average temperature in the air gap [K]
θ_{ope}	surface temperature of the external side of the PV module [K]
θ_{opi}	surface temperature of the external side of the facing wall [K]
θ_{out}	outlet air temperature [K]
θ_{se}	surface temperature of the air gap side of the PV module [K]
θ_{si}	surface temperature of the air gap side of the facing wall [K]
ϕ_{se}	thermal energy flow through the external surface layer [W/m^2]
ϕ_{si}	thermal energy flow through the internal surface layer [W/m^2]

it was emphasised that standard test procedures, as described in IEC 61215 [5], are not directly applicable for BIPV systems.

The later EC IMPACT project [6] (1998–2000) studied the heat exchange of a PV module to its surroundings and the first version of an outdoor Test Reference Environment (TRE) for double skin applications of BIPV systems was built at the EC Joint Research Centre (JRC) of Ispra. The TRE was used to assess the thermal exchange of a PV module within the building envelope. The purpose of the experimental work on TRE was to obtain several data series for the same PV module under different boundary conditions and to compare them with data series from other PV modules. Reference mini-modules were specifically designed during this project, for testing the performance of similar PV module composition in fully insulated and free-rack conditions [7]. Several numerical models were developed by different authors [8–11] based on experimental data from the initial and improved version of the TRE.

A third and further improved version of the TRE was built in 2009 by the International Centre for Numerical Methods in Engineering (CIMNE) and the University of Lleida (UdL) [12]. One of the most relevant improvements is the support structure which allows any inclination of the PV module to be tested, varying from horizontal to vertical. In Lleida, the energy performance of the PV module placed at the TRE opening is compared with that of two identical PV modules used as a reference, one fully insulated and the other under free-rack conditions. From the experimental campaign of the TRE of Lleida, other models have been developed by Lodi et al. [13].

From the experience gained with the 10-year experimental and modelling work on the TRE, this paper presents a proposal for a common Test Reference Environment for double skin BIPV systems. This paper proposes harmonised requirements and recommendations in order to define a common procedure for testing double skin BIPV systems in a well-controlled Test Reference Environment, thus providing suitable input for design and modelling work.

The recently started IEA ECBCS Annex 58 [14] offers the possibility to further develop practical solutions for BIPV double skin applications through outdoor testing and dynamic analysis methods.

2. BIPV and harmonisation

3.1

For a good understanding of the applications of PV in the built environment that are presented here, it is important to distinguish between the following applications:

- PV rooftop and PV cladding façade applications use the building for the support structure while an impact on the energy system is not considered.
- BIPV covers PV technology integrated in the building envelope (roof or façade) giving impact to the overall energy behaviour and functionality of the building such as a roof construction element. Thus BIPV covers the application area where PV technology is an integral part of the energy system of the building.
- PV/T is the technology of a separate system that produces both electrical and thermal energy which can be utilised in a building and could be integrated in the building envelope as well.

Sometimes the terminology of hybrid PV is used; following the definition by ESRU [15], hybrid PV components in the built environment are building elements in which the integration of PV technology not only serves for electricity production, but where the thermal impact of the elements is also used for other purposes.

Building designers are interested in the performance under operating conditions for a typical climate, season and specific location taking into account the energy use of their design. Integration of PV in the building envelope implies that they not only have to take into account electrical energy production, but also thermal (avoiding overheating in summer) and comfort (daylight, ventilation and quality of air) aspects. A further consideration is that building designers need performance indicators based on climatic variables: ambient temperature, solar radiation, wind velocity and site dependent data such as obstructions giving possible shading problems.

PV components, integrated in a building's envelope, interact with the building in many respects. This is schematically shown in Fig. 1. A comprehensive assessment procedure should include the following aspects:

- Electrical performance
- Thermal processes at component level
- Seasonal dependency of the thermal performance
- Ventilation performance
- Visual performance

Please cite this article in press as: J.J. Bloem, et al., An outdoor Test Reference Environment for double skin applications of Building Integrated PhotoVoltaic Systems, Energy Buildings (2012), doi:10.1016/j.enbuild.2012.03.023

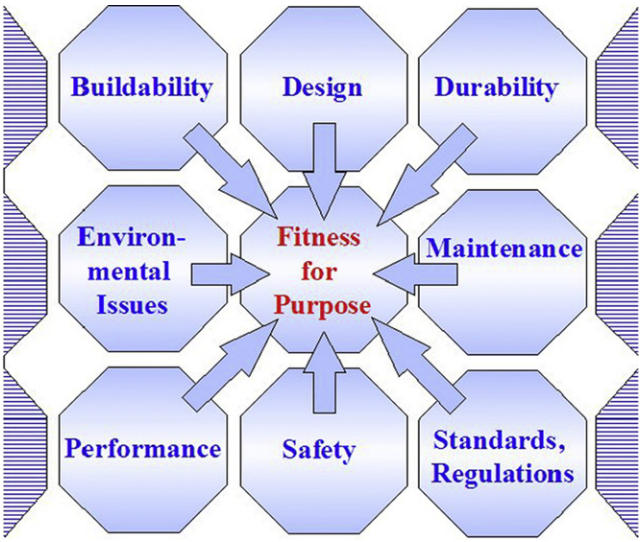

Fig. 1. Schematic presentation of different aspects for PV building integration [16].

- Maintenance related aspects and durability
- Other performance objectives

Aspects related to the electrical, thermal and ventilation performances are schematically presented in Fig. 2 and briefly described below.

2.1. Electrical performance of BIPV elements

The measurement of the electrical performance of PV elements has already been standardised to a large extent. The electrical efficiency, however, is dependent on the temperature of the PV element. If the absorbed solar heat is partially recovered for other purposes in a hybrid component, then this will affect the electrical efficiency due to the temperature coefficient of the active material. The main technology is that of wafer-based silicon PV cells (85% in 2010 [17]), which is used in most common PV modules and has a negative temperature coefficient. Therefore a combined thermal and electrical performance test in real outdoor conditions is necessary. With the PV-Hybrid-Pas project [2], outdoor test cells were used for a calorimetric assessment of a PV system under double skin conditions. During the IMPACT project [6], the TRE was used to assess the thermal exchange of the PV module with its immediate environment.

2.2. Thermal processes at component level

The following aspects are to be investigated:

- Dynamic aspects of heat transfer through the component in the situation without airflow in the cavity. The heat transfer is complex and is further described in.
- Overall energy performances for the test duration but also for standardised conditions. This requires the combination of realistic measurements with simulations, through so-called scaling and replication techniques.
- Dependency on component dimensions. The thermal buoyancy effects (and therefore also the electrical efficiencies) vary as function of the size (height) of the PV installation.

2.3. Thermal performance in winter and summer

The heat gained by PV modules solar absorption can be used for heating purposes of the spaces adjacent to these PV facades or roofs. The interaction with the space can be studied by outdoor testing of the component in test cells. Based on the results of the outdoor experiments, the effect of such components on real buildings and in various climates can be studied by simulation (scaling and replication) of the energy, ventilation and daylight performance. The thermal comfort in an adjacent room can also be evaluated [18].

The pre-heating of air under BIPV conditions is not always an advantage. In summer period, pre-heated air may have a negative influence on the indoor climate. In practice, different ventilation strategies of the cavity for the summer and winter period are therefore required.

In addition, in the case of semi-transparent PV elements, heat flows can pass through the inner surface of the building component (partly direct solar gains, partly by radiation due to the high surface temperature). This is an important effect, which is included in the evaluation.

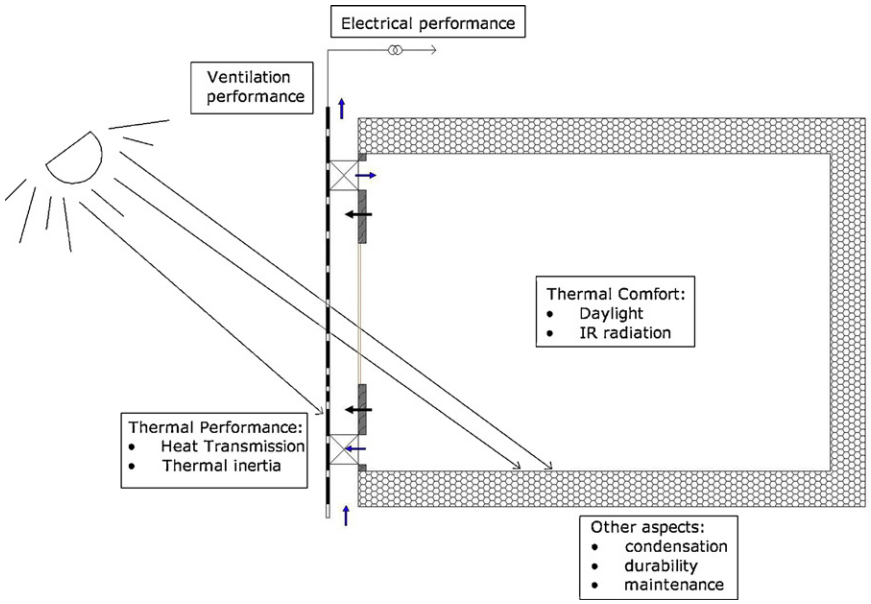

Fig. 2. Interaction of various phenomena for a PV component applied to a building envelope.

Please cite this article in press as: J.J. Bloem, et al., An outdoor Test Reference Environment for double skin applications of Building Integrated PhotoVoltaic Systems, Energy Buildings (2012), doi:10.1016/j.enbuild.2012.03.023

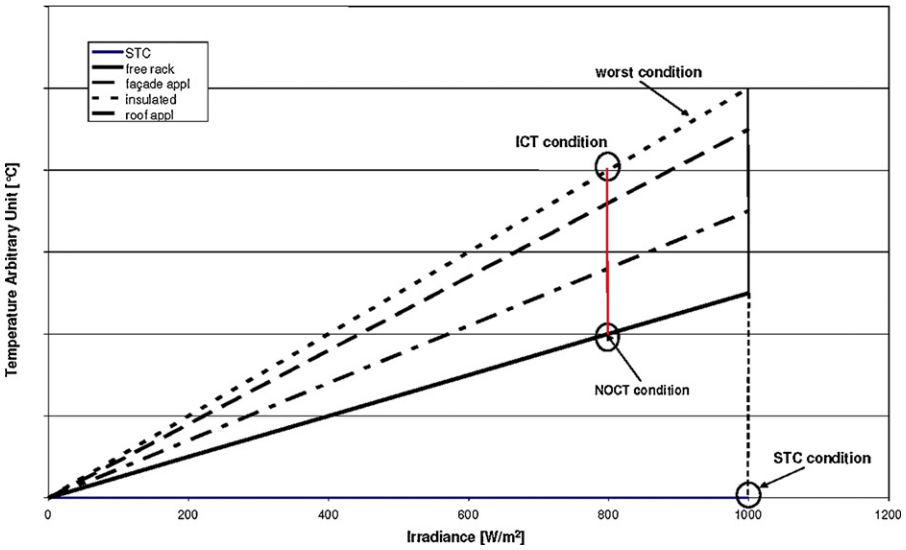

Fig. 3. Temperature difference versus irradiance [22].

2.4. Ventilation performance

The utilisation of warm air for the purpose of pre-heating, in particular for the colder season, needs an assessment of the ventilation performance of the integrated PV-installation. With respect to the procedures for evaluating the ventilation performance, a distinction must be made between two types of systems:

- Naturally ventilated systems. The airflow rate varies over time as a function of the outside climate, the inside climate and the use of the building. Prediction of the performance is complex.
- Mechanically driven systems. In this case, the airflow rate should be more or less constant and known. The estimation of the thermal balance is therefore easier to make.

The technical data provided by the PV industry are based on standardised measurements under laboratory conditions described in IEC 61215 [5].

The most important test procedures are:

- 10.2 Standard Test Conditions (STC),
- 10.5 Measurement of Nominal Operating Cell Temperature (NOCT),
- 10.6 Performance at NOCT,
- 10.7 Performance at low irradiance.

Concerning 10.5, NOCT is defined as the equilibrium mean solar cell junction temperature within an open-rack mounted module in the following Standard Reference Environment (SRE):

- Tilt angle: at normal incidence to the direct solar beam at local solar noon
- Total irradiance: 800 W/m^2
- Ambient temperature: 20 °C
- Wind speed: 1 m/s
- Electrical load: 0 A (open circuit, thus no current flowing)
- Open rack mounted PV modules with optimised inclination.

Measurement of NOCT for PV modules applied as BIPV components are of most interest as the negative temperature effect on the maximum power is about 0.5%/°C (referred to conditions at 25 °C).

A number of different circumstances occur when PV modules are applied as integrated components in a building, which is far from the Standard Reference Environment as described in the IEC 61215:

- The inclination for façade application is typically 90°, and for roof applications it depends on the roof construction but is seldom optimised.
- Free convection at the rear side of the PV modules does not occur.

As a consequence the most notable differences are in level of irradiation and operating cell temperature. Therefore conversion from PV module specifications at Standard Test Conditions (25 °C, 1000 W/m^2, air mass 1.5 Global) to BIPV applicable electric system design values is of highest priority as the integration of PV in buildings continues to emerge. The conversion from STC to outdoor open rack conditions is studied in [19] and indicates an error of about 2% for p-Si PV-modules. It is common to illustrate the thermal and radiance relation in a graphical way as shown in Fig. 3 where the temperature difference between the PV module and ambient is plotted against the solar irradiance.

All BIPV applications differ from the conditions described above. The main differences are to be found in the convective and radiative heat exchanges on the rear side of the PV module. These different

Fig. 4. Different BIPV conditions: integrated roof (top), ICT reference device (on the left) and ventilated reference device (on the right) [7].

Please cite this article in press as: J.J. Bloem, et al., An outdoor Test Reference Environment for double skin applications of Building Integrated PhotoVoltaic Systems, Energy Buildings (2012), doi:10.1016/j.enbuild.2012.03.023

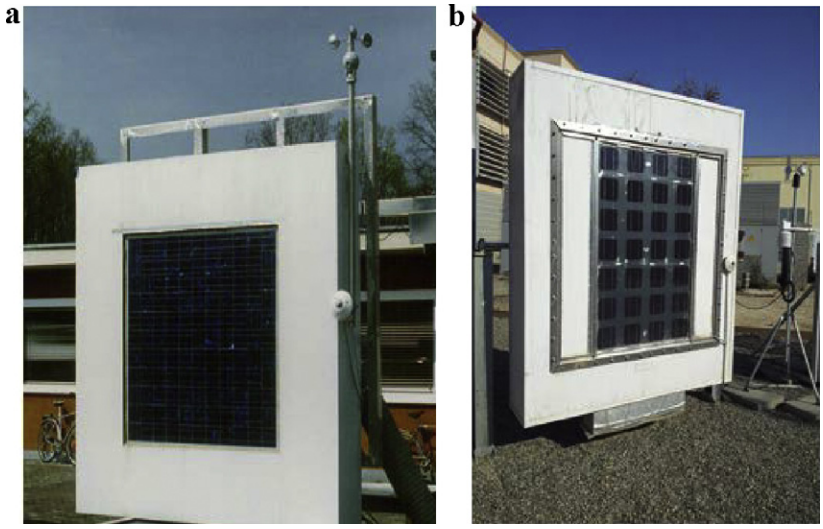

Fig. 5. Front view of the previous experimental set-up. (a) TRE at the JRC in Ispra, Italy; (b) TRE at the PCiTAL in Lleida, Spain.

thermal exchanges cause the NOCT line to move upwards in Fig. 3. Thus even if the NOCT – SRE are available, the outdoor surroundings may cause a different equilibrium mean solar cell junction temperature due to different ground reflectances (from asphalt, grass, grit, etc.) and convective heat exchanges.

In Fig. 3 the standardised reference points are given, according to the STC and NOCT conditions. From the graph, it can be concluded that building integrated PV applications are situated above the NOCT line. The worst condition is when the PV module does not have convective or radiative thermal flows at the rear side. This experimental situation has been created by insulating a PV module with 10 cm of expanded polystyrene. The measurement conditions performed with this specific module, shown in Fig. 4, are referred to as Insulated Test Condition (ICT). Since standard or guidelines for measurement do not exist at present for these conditions, designers and architects need to calculate with extrapolated data from specifications based on STC and NOCT data supplied by PV module manufacturers. An ICT reference device can assist in defining the worst PV application condition. This device has been developed and used by the JRC in several EU research projects and experiments [7].

3. Testing

A proposal for a Test Reference Environment for double skin BIPV applications is presented.

The first version of a common Test Reference Environment for BIPV systems was designed and built at the EC JRC of Ispra during the IMPACT project in 2001. The experimental set-up is shown in Figs. 5 and 6. It is composed of a wooden box with external sizes of 203 × 203 × 46.5 cm in order to be positioned at the opening of a PASLINK test cell [3]. The internal south-oriented TRE opening allowed the positioning of PV modules with the maximum sizes of 120 × 120 and 3 cm thickness. From the bottom, air could enter and be extracted from the top by means of 20 cm diameter tubes. The air inlet and outlet sections were initially placed behind the wooden box in order to make caloric experiments possible as a design option for the PASLINK test cell.

3.1. Experimental set-up of the previous Test Reference Environment for double skin BIPV systems in Ispra and Lleida

The initial measurement set-up is shown in Fig. 7. Several temperature sensors (thermocouples) were placed in correspondence of the inlet and outlet sections of the air cavity and at three different heights on both sides of the insulation layer. No additional sensors were initially placed in correspondence of the PV module surface since the reference PV module contained specific cells to measure the Voc corresponding temperatures and Isc corresponding irradiation.

Different experiments were carried out within the first TRE set-up, testing different PV module compositions under several air flow rates and studying the effect of aluminium transversal fins of 5 cm length over the air gap rear-facing surface. Dedicated PV modules were also designed [20]. Reference mini-modules were also

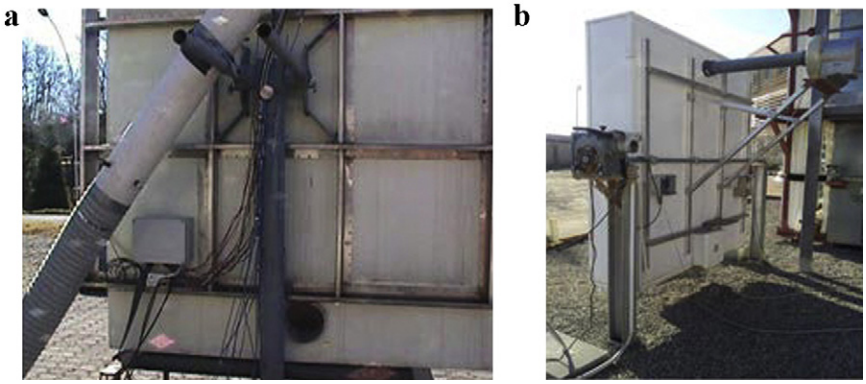

Fig. 6. Rear view of the previous experimental set-up. (a) TRE at the JRC in Ispra, Italy; (b) TRE at the PCiTAL in Lleida, Spain.

Please cite this article in press as: J.J. Bloem, et al., An outdoor Test Reference Environment for double skin applications of Building Integrated PhotoVoltaic Systems, Energy Buildings (2012), doi:10.1016/j.enbuild.2012.03.023

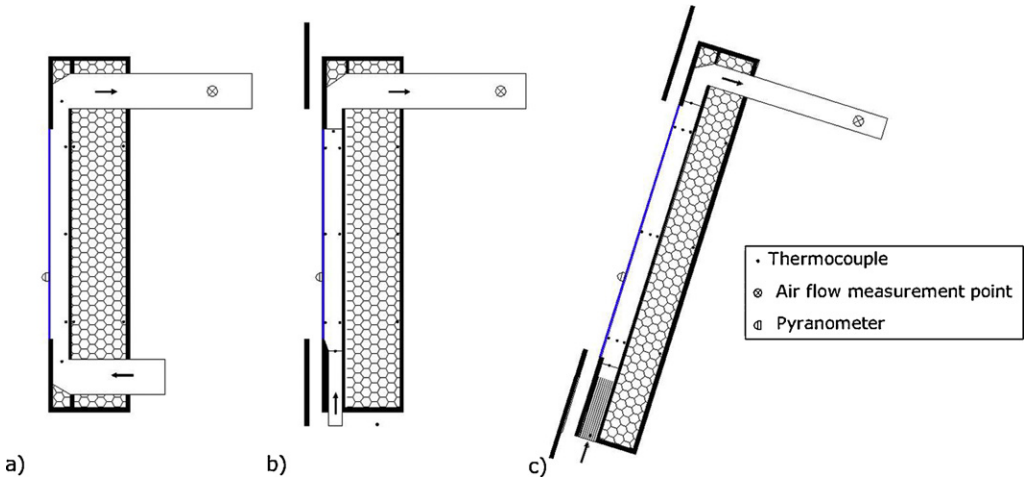

Fig. 7. Lateral cross-section of the previous TRE measurement set-up. (a) First version; (b) second version; (c) third version (variable inclination).

designed for testing the performance of similar PV module compositions in fully insulated and free-rack conditions. Three variables were measured by the device: the irradiation level by measuring the short-circuit current (Isc) over a precision resistance, the open voltage (Voc) and the difference between ambient and PV cells temperature. In Fig. 8 the design of a reference mini-module is shown [7].

Improvements were made to the first TRE set-up. Regarding the geometry, the air-inlet tube was substituted by a 0.1 m^2 rectangular opening to guarantee a non disturbed airflow entrance, reducing the measurement uncertainty. During the IMPACT project, JRC laboratory measurements have shown the need for using honey comb at the inlet entrance. In order to avoid shading effects due to the frame, the PV module was mounted in line with the white painted façade. External shading devices were placed in correspondence to the air-inlet and outlet to avoid effects of disturbance from solar radiation. Several temperature sensors were also placed in correspondence to the PV module internal surface at three levels (see Fig. 7).

A third version of the TRE was built in 2009 at the Lleida Outdoor Test centre (LOTCE) of the CIMNE-UdL located in the Lleida Agrifood Science and Technology Park (PCiTAL). Some improvements were made to the experimental set-up, like the new support structure, which allows for any inclination of the PV module to be tested, varying from horizontal to vertical. In addition, the fan was placed at the same height as the outlet tube, reducing corner effects. An array of plastic made cylindrical tubes of 0.5 cm diameter was placed at the air inlet in order to guarantee a non-disturbed flow pattern (see Fig. 7).

With this third set-up, additional experiments were made testing different materials at the rear-facing surface with the same semi-transparent PV module configuration. The tested materials include a black absorber sheet, a white diffuse reflector sheet and an aluminium specular reflector sheet. Furthermore, several airflow regimes for different PV module inclinations were tested [12].

3.2. Description of a standard set-up for a Test Reference Environment

Feedback from 10-year experimental and modelling work on TRE led to the proposal of a standardised set-up for a Test Reference Environment for double skin applications of BIPV. An impression of the outdoor Test Reference Environment set-up is given in Fig. 9, where the fully insulated mini-module is positioned on the left and

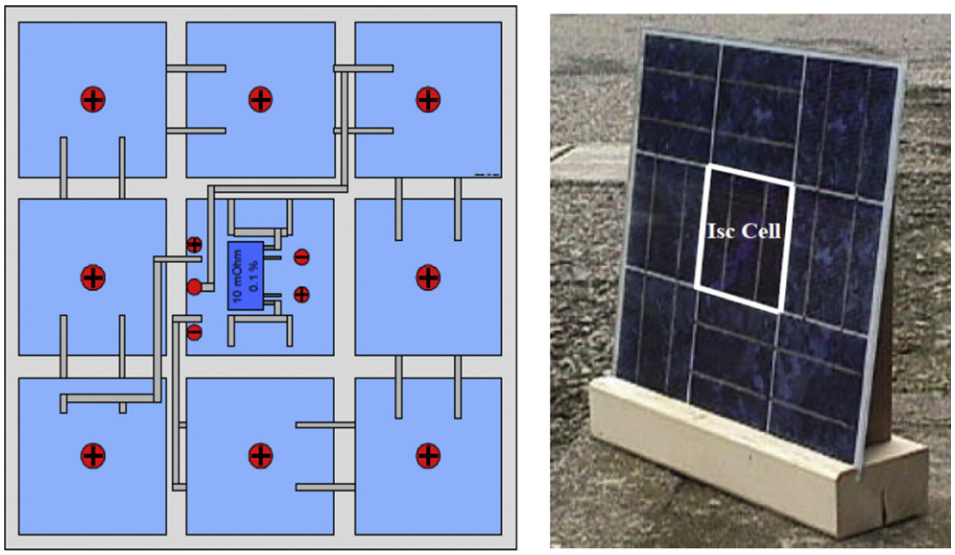

Fig. 8. Design of a reference PV mini-module [7].

Please cite this article in press as: J.J. Bloem, et al., An outdoor Test Reference Environment for double skin applications of Building Integrated PhotoVoltaic Systems, Energy Buildings (2012), doi:10.1016/j.enbuild.2012.03.023

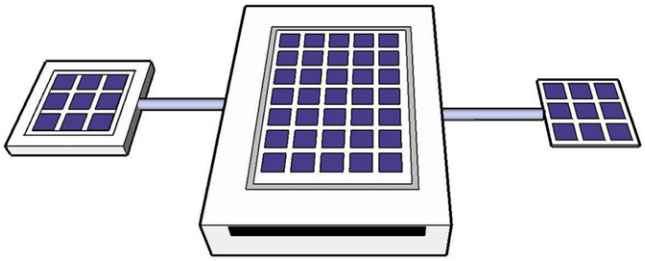

Fig. 9. Schematic presentation of the presented Test Reference Environment and reference mini-modules.

the free-rack mini-module on the right. Below an explanation is presented on geometry, instrumentation, experimental set-up and calibration issues.

3.2.1. Geometry

Requirements for the TRE geometry and materials are given below.

The south-oriented opening should allow the positioning of PV modules with maximum sizes of 1.2 × 1.2 m. The weather resistant wooden box should be made by white-painted wooden panels (from 1.5 to 3 cm thick). In order to take on adiabatic conditions behind and to the lateral sides of the air channel, the insulation layer of the box should be at least 30 cm thick of expanded polystyrene (EPS) (thermal conductivity 0.032–0.037 W/mK). The error due to the conduction of these layers is less than 0.5%.

The support structure should allow any possible inclination to be tested (from 15° to vertical). The air is extracted from the top by means of a variable speed fan in order to test different air gap flow rates.

The PV module has to be mounted in line with the façade to avoid shadowing effects. Adjustable external shading devices are recommended in correspondence of the air-inlet and outlet to avoid effects of disturbance from solar radiation. The shading devices may be white painted aluminium panels with sizes of 1.2 × 0.4 m in order to protect the inlet entrance. The distance from the TRE wooden box should be around 4 cm.

The air should enter from the bottom by means of a rectangular entrance section of dimension 120 × 10 cm; a honey comb structure is recommended to guarantee a laminar air inlet pattern flow.

It is recommended to install a small inclined roof on the top of the box to avoid water stagnation or infiltration that could reduce disturbance from solar radiation as well.

3.2.2. Instrumentation

In general, to reduce the resulting error from analysis, the highest attention has to be given to sensor measurement accuracy and its positioning. The measured signal has to represent the physical meaning and should correspond with model input, therefore disturbance from solar radiation should be avoided by shielding temperature sensors. A weather station nearby could provide important data for analysis, such as temperature, solar radiation, wind speed and direction and relative humidity but these data should be applied for control or back-up purposes only. In principle, all required input data for the analysis process has to be measured next to the TRE.

The following requirements are considered for the TRE instrumentation and sensors:

- Surface temperatures of the PV module and the rear-side material have to be measured at least at three different heights (in correspondence to the bottom, top and middle of the air cavity). For the PV cells temperature it is preferable to measure in the centre of the cell to avoid border effects. Recommended contact sensors are stick-on type T thermocouples or PT100 (minimum accuracy of 0.3 °C).
- Air gap temperatures have to be measured at least at three different heights (in correspondence to the bottom, top and middle of the air cavity) (see Fig. 10). Cylindrical shading protections should be used in correspondence of these sensors to avoid effects from direct solar radiation. It is suggested to use thermocouple piles to measure the temperature difference between inlet and outlet section corresponding to the bottom and top of the PV module. Recommended sensors are type T thermocouples. Special small devices (like copper plates of 1 cm^2) may be placed to give some thermal mass to the sensors to obtain a smoother temperature reading. Additional air temperatures can be measured in the outlet tube by an array of thermocouples.
- Regarding the air flow rate measurements, it is strongly recommended to follow a standardised method for air flow measurements in tubes [12]. For the correct application of this method, the straight outlet duct should have a length of at least 5 times the diameter before the measuring section. Regarding the air velocity measurements, it is recommended to use omnidirectional hot wire anemometer for air velocity lower than 0.4 m/s and miniature cup anemometers for higher speeds.
- It is recommended to use a calibrated pyranometer for the solar irradiance measurements. The pyranometer has to be placed in line with the façade and preferably at middle height of the PV module. The minimum resolution required is 1% of the readings.
- Ambient air temperature has to be measured with ventilated sensors shielded from solar radiation; it is preferable to measure at least in two different positions in respect to the TRE: behind, in the shading of the TRE wooden box and in correspondence to the air inlet section. Measuring the ambient temperature at several positions would guarantee the measurement of the correct signals that correspond to the energy flows due to the BIPV system boundary conditions. Some thermal mass could be given to these sensors.
- Wind direction and speed might be measured with a cup-type anemometer placed about 5 m in front of the TRE and at PV module level (2 m height).
- Electricity production: three different possibilities are considered:
  - PV module connected with a micro-inverter;
  - PV module connected with an MPP tracker;
  - PV module that enables switching from Voc to Isc with a special

electrical circuit (*I–V* curve generation); it is preferable to have the PV module designed in such a way that it contains specific cells in open circuit (to track also the PV cells temperature), and in short circuit (for the additional assessment of the absorbed solar irradiance).

3.2.3. Experimental set-up

Data have to be recorded with 1-min intervals in order to study the dynamic effects from solar radiation and wind.

A minimum test period of 24 h is required, thus including the night time period. In this way the energy balance during the night can be assessed as well. Selected days for evaluation have to fulfil several requirements. Series of days with similar solar irradiance distribution but different temperatures and wind speeds have to be considered for assessment purposes. Both sunny and cloudy days have to be considered.

Since data from test-days should contain enough information, a minimum incident solar energy of 5 kWh, during one day and at the same inclination of the PV module, has to be reached for the acceptance of the test. During this measurement period, wind speed should be stable enough: data could be averaged at 8-h intervals during one day period and if the average values differ more than

Please cite this article in press as: J.J. Bloem, et al., An outdoor Test Reference Environment for double skin applications of Building Integrated PhotoVoltaic Systems, Energy Buildings (2012), doi:10.1016/j.enbuild.2012.03.023

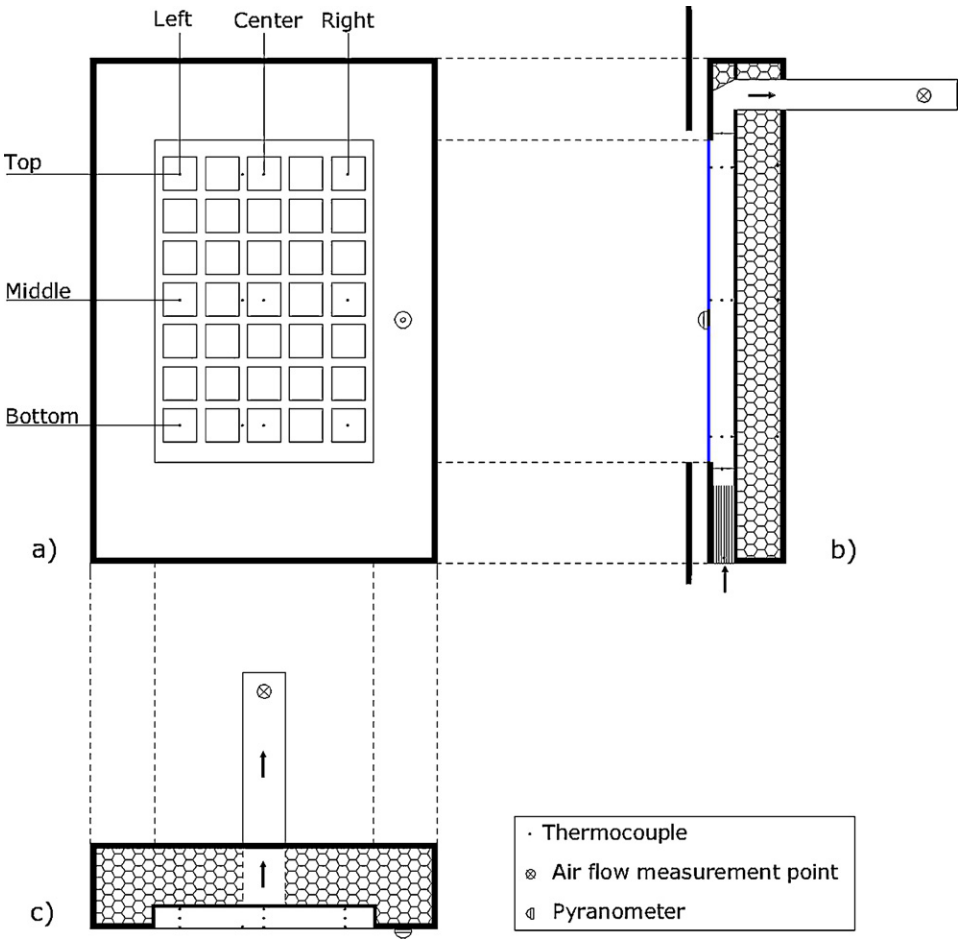

Fig. 10. Sensor positioning of the presented standard Test Reference Environment. (a) Front view; (b) cross view; (c) top view.

90% within the same day, the test has to be considered as a special case for the analysis.

3.2.4. Calibration issues

Several experiments have been carried out at the JRC to assess calibration information for the TRE. These include the use of heating foils to simulate the temperature pattern of a PV module (and rear-side material) under laboratory conditions.

Transparent plexiglass may also be used to substitute the PV module under laboratory conditions to measure airflow patterns and air velocity with a hot wire anemometer. These measurements give an impression of the flow and disturbance of the inlet air and reveal the necessity to use honey comb in the entrance.

It is recommended, when possible, to produce reference mini-modules and apply them during the experimental outdoor testing [7].

4. Evaluation of the experimental data

2.2

The data collected during the experimental tests give input to the evaluation work.

A proper check of the measured data for unexpected observations is required and if necessary may be filtered in time and space in order to be used as input signals for analysis. Simple graphical representation of the signals may indicate any inconsistency. Mathematical evaluation techniques intend to identify unknown parameters by means of comparing measured and modelled output. It is an approach where a model is fitted to the input data by identifying suitable values to its parameters [21]. The first step of the evaluation process is to determine an appropriate mathematical model, based on the energy balance of the system and the available data.

4.1. The energy balance

The different energy flow processes which occur when the double skin BIPV system is exposed to solar radiation are shown in Fig. 11.

The evaluation of the different energy flow processes within the system leads to the definition of three distinctive energy balances, which refer to three energy exchange layers of the system, the PV module, the air gap and the opaque rear-facing material.

Considerable temperature differences occur between the upper and lower part of the three exchange layers [9,12]. It is therefore preferable to consider three vertical levels for the energy balance of the BIPV system [9,11], as shown in Fig. 12.

The energy balance within each vertical layer can be done considering spatially uniform wall temperature (UWT) or spatially uniform heat flux (UHF) boundary conditions for the solid surfaces. Regarding the energy balances at each energy exchange layer, the assumption of the lumped capacitance method is acceptable (see [10,11]) This assumption is recommended when the conductivity of the PV module is negligible and high resolution data are not available. It is also possible to consider more detailed analysis based on finite differences or finite elements to model the heat conduction within the solid layers. However, since the vertical temperature distribution within the layers of the system is not negligible and it

Please cite this article in press as: J.J. Bloem, et al., An outdoor Test Reference Environment for double skin applications of Building Integrated PhotoVoltaic Systems, Energy Buildings (2012), doi:10.1016/j.enbuild.2012.03.023

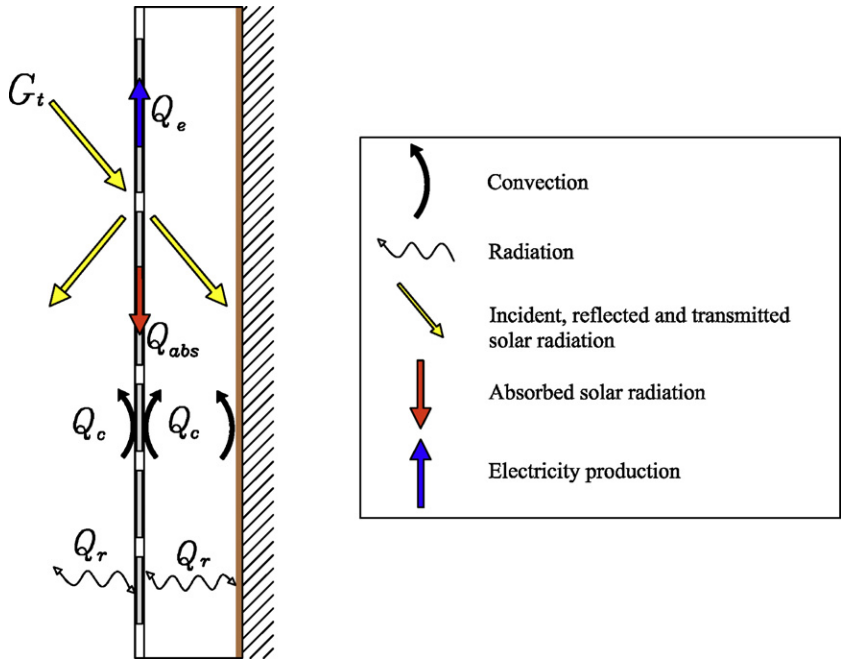

Fig. 11. Schematic view of the different energy flow processes within TRE.

is normally non linear, both UWT and UHF boundary conditions are approximations of the reality.

It follows the overall energy balance equations for each layer of the system, considering the electrical analogy model [22]:

1. Energy balance for the air gap

$$\dot{m}c_p(\theta_{out} - \theta_f) = A\,h_{cv1}(\theta_{se} - \theta_{int}) + A\,h_{cv2}(\theta_{si} - \theta_{int}) \quad (1)$$

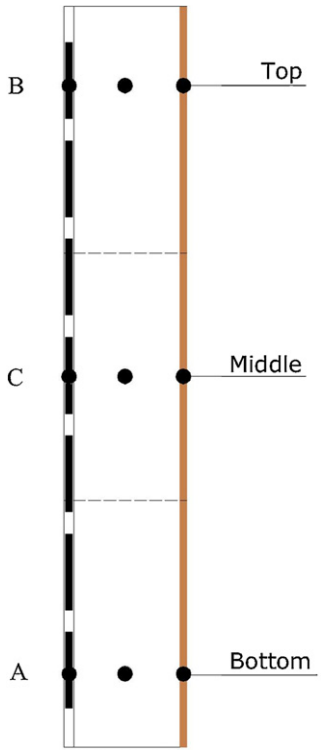

Fig. 12. Scheme of the estimation set-up.

2. Energy balance for the external surface of the air gap

$$\varphi_{se} = \frac{(\theta_{ope} - \theta_{se})}{R_e^*} + N_i^* \alpha_{est}\, G_t = \frac{(\theta_{se} - \theta_{int})}{R_{cv}} + \frac{(\theta_{se} - \theta_{si})}{R_{rd}} \quad (2)$$

3. Energy balance for the internal surface of the air gap

$$\varphi_{si} = \frac{(\theta_{int} - \theta_{si})}{R_{cv2}} + \frac{(\theta_{se} - \theta_{si})}{R_{rd}} = \frac{(\theta_{se} - \theta_{opi})}{R_i^*} \quad (3)$$

4.2. Uncertainty of parameters

Some parameters are not exactly known in the energy balance and give a relative high contribution to the energy balance, such as the convective heat exchange coefficients and the solar absorption. Special attention is paid to the identification of the convective heat transfer exchange coefficients within the air gap. These parameters can be determined with literature correlations [23–27] however, they are difficult to define, especially for laminar flow.

The convective heat transfer coefficient at the exterior surface of the PV module is normally defined as a linear or exponential function of wind speed [28–30], but only for high wind speed.

Regarding the solar absorption of the PV module, especially if a semi-transparent PV module is tested, it is important to distinguish between the absorption of the opaque (PV cells) and the transparent area by considering two different values [9] or an equivalent weighted value for α_{est}. In order to take into account the reflective properties of the external surface of the PV module, the solar absorption can be expressed as a function of the angle of incidence [31]. It is also possible to take into account internal reflections with the net transfer method [32].

4.3. Recent analysis work with data from TRE

Different authors [10,11,13] developed identification models that fit the data by identifying suitable values to the aforementioned physical parameters of the system.

Jiménez et al. [10] developed several grey-box models for the energy transfer evaluation of a double skin BIPV façade based on experimental data from the second version of the TRE. The outweighing factor of grey-box models is the possibility to combine

Please cite this article in press as: J.J. Bloem, et al., An outdoor Test Reference Environment for double skin applications of Building Integrated PhotoVoltaic Systems, Energy Buildings (2012), doi:10.1016/j.enbuild.2012.03.023

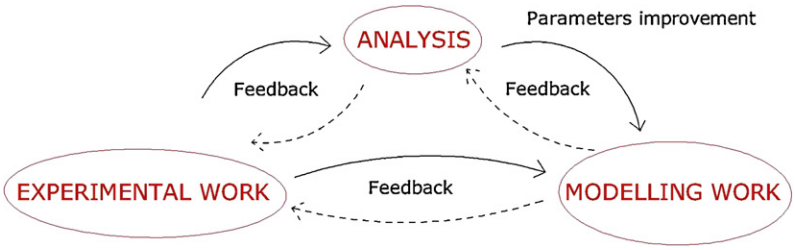

Fig. 13. Overview of the processes involved in the assessment of the energy performance.

prior physical knowledge of the system and statistics. The temperature of the PV module was chosen as the state and the output variable and different linear and non-linear models were presented. It was found that a non-linear single-state model was the most suitable for describing the dynamics convective and radiative of the BIPV energy balance.

In [11], the model formulated in [10] was applied with different experimental data from the second version of the TRE, where transversal fins were placed in the air gap. Within this work, an exponential relation between the wind speed and the ambient convective coefficient was correctly identified for the specific set-up.

Lodi et al. [13] developed an extension to the models described in [11], identifying several convective heat exchange coefficients for different air flow rates using non-linear grey-box models based on experimental data from the third version of TRE. The identified Nusselt numbers are in the range of 10–90 for Reynolds numbers varying from 1000 to 30,000.

5. Prediction and modelling work

Modelling work intends to predict output data from validated models with identified or assumed parameters. Mathematical modelling work is used to describe the dynamic behaviour of a phenomena or a process.

Over the last 10 years, the experimental data from TRE has been used for validation of modelling work by several academic groups.

5.1. Recent modelling work with data from TRE

Starting from the first version of TRE in Ispra, Italy, Christ [8] compared simulation results using ESP-r. Experimental data from this first version of TRE were compared with data from two different PV-Hybrid-Pas test cells located in Stuttgart, Germany and in Athens, Greece. The developed program used the air gap heat exchange coefficients from literature. When predictions did not correspond with the experimental data, a set of heat transfer coefficients was assessed by a parameter fitting and optimisation technique. The conclusions of the author were that simulations of high laminar flow using heat transfer coefficients calculated with standard correlations seem to deliver appropriate predictions as long as the temperature differences between the PV module and the air are lower than 35 °C. For lower airflow rates and higher temperature differences, the actual heat transfer coefficients were found higher than the calculated ones probably because of the higher uncertainty. Therefore a more detailed study of the convective heat exchange coefficients was planned for future work.

Experimental data from the first version of TRE were used also by Gandini [9,22] to validate a new TRNSYS model. An electrical analogy model which includes the PV module conduction resistance was used. Within this study, data from tests carried out over 4 different PV modules under several air flow rates were tested. In order to investigate the heat transfer coefficients within the air gap, a three-dimensional model of the air gap was developed using FLUENT 6.2.0 software, giving adjusted parameters for the analysis process. The model showed a good agreement with the measured values of θ_{se}, while for θ_{si} a disagreement was found between predicted and measured values. An error of less than 5% was found in the prediction of the electricity production. It was found that the air inlet tube created strong local turbulences that locally increased the convective heat transfer coefficients.

Based on these results, several changes of the TRE geometry and set-up were considered and implemented for improved experiments and high quality data.

Based on the third version of the TRE experimental data, Cipriano [32,13] validated another TRNSYS model. UHF boundary conditions were considered in this work and a single control volume was established for the energy balance within the air gap. The heat conduction within the solid layers was modelled using a one dimension finite element discretisation approach and 10 nodes were considered for each energy exchange layer. A first validation was carried out in [13], thus a more precise refinement of the convective heat exchange coefficient correlations was necessary.

It is important that the model developed for double skin applications of BIPV systems should be integrated with the model of the overall building in order to analyse the feasibility of the investment. The procedure for investigating the ability to model the test component is divided into three stages: calibration (alignment of the test component simulation model with experimental data), scaling (simulation of a full-scale building with the building component, using the "Integrated Performance View [18]" standardised calculation) and replication (repeating the simulations with different locations). Within the outlined procedure, the assumption that the simulation program is capable of modelling all aspects of the building is done. Therefore, within the validation process, this assumption is verified.

5.2. Feedback between evaluation and modelling work

The evaluation and modelling processes should provide a reciprocal feedback to each other for high quality performance characterisation. In fact, results from evaluation can be an input for model validation work but also modelling work gives input to evaluation for model optimisation and for a proper design of the experimental work (see Fig. 13). This approach has led to the third and improved version of the TRE and to the definition of an harmonised set-up.

6. Conclusions and recommendations

After more than 10 years of development in different European research projects, a standard Test Reference Environment for double skin applications of BIPV Systems is presented in this paper. Using this reference environment for PV modules integrated in facades or roofs, different PV module configurations can be tested changing the boundary conditions. The paper suggests also a common way of evaluating the data obtained from the experiments. Mini-modules are proposed to get the required information for

Please cite this article in press as: J.J. Bloem, et al., An outdoor Test Reference Environment for double skin applications of Building Integrated PhotoVoltaic Systems, Energy Buildings (2012), doi:10.1016/j.enbuild.2012.03.023

evaluation. These modules give an indication of the BIPV performance range, introducing an additional point for reference. The first version of the TRE was developed during the IMPACT project and improvements were made during the last 10 years at the JRC and Lleida. Several thermal processes are considered in the energy balance and several non-linear parameters are identified by estimation. Important improvements in the controlled outdoor experimental set-up and data evaluation have been made based on identifying from analysis and modelling work. Different authors successfully developed numerical models, using experimental data from the TRE and an overview of the most important results is presented as well.

In order to harmonise experimental work for the assessment of electrical as well as thermal characteristics of photovoltaic systems in the building envelop, it is recommended to define a common outdoor test environment as a proposal is presented herewith. Presently the definition and assessment of electrical performance data is defined in IEC standards but do not cover BIPV applications. Harmonisation could be further developed in EU projects to support the definition of international standards.

The definition of an Insulated Test Condition for PV modules as described in this paper would support the indication of the performance range for BIPV applications. The ICT point could be inserted into the IEC 61215, which now includes only STC (laboratory conditions) and NOCT (free-rack mounted conditions) points.

Acknowledgement

This work is financially supported by a grant of the Spanish Ministry of Science and Innovation, FPU program (ref. AP2008-01801).

References

[1] European Parliament, Directive 2010/31/EU of the European Parliament and of the Council of 19 May 2010 on the energy performance of buildings, 2010.
[2] D. van Dijk, R. Versluis, PV-HYBRID-PAS: results of thermal performance assessment, in: Proceedings of the 2nd World Conference and Exhibition on Photovoltaic Solar Energy Conversion, Vienna, Austria, 1998.
[3] P.H. Baker, H.A.L. van Dijk, PASLINK and dynamic outdoor testing of building components, Building and Environment 43 (2008) 143–151.
[4] J.C. Jol, J.J. Bloem, B.M. Cross, M. Sandberg, K. Wambach, W. Wiesner, et al., Towards a CE mark for PV building integrated systems, in: Proceedings of the 16th European Photovoltaic Solar Energy Conference, Glasgow, UK, 2000.
[5] International Standard IEC, 61215, Crystalline Silicon Terrestrial Photovoltaic (PV) Modules – Design Qualification and Type Approval, 2005.
[6] J.R. Bates, U. Blieske, J.J. Bloem, J. Campbell, F. Ferrazza, R.J. Hacker, et al., Building implementation of photovoltaics with active control of temperature, in: Proceedings of the 17th European Photovoltaic Solar Energy Conference, Munich, Germany, 2001.
[7] J.J. Bloem, The JRC PV reference module for an energy rate indicator, in: Proceedings of the 16th European Photovoltaic Solar Energy Conference, Glasgow, UK, 2000.
[8] F.H.M. Christ, Comparison of measured and predicted data for PV hybrid systems, Master's thesis, University of Strathclyde Department of Mechanical Engineering, 2001.
[9] A. Gandini, Analisi numerica delle facciate fotovoltaiche a "doppia pelle", Politecnico di Milano, 2003.
[10] M.J. Jiménez, H. Madsen, J.J. Bloem, B. Dammann, Estimation of non-linear continuous time models for the heat exchange dynamics of building integrated photovoltaic modules, Energy and Buildings 40 (2008) 157–167.
[11] N. Friling, M.J. Jiménez, J.J. Bloem, H. Madsen, Modelling the heat dynamics of building integrated and ventilated photovoltaic modules, Energy and Buildings 41 (2009) 1051–1057.
[12] C. Lodi, J. Cipriano, J.J. Bloem, D. Chemisana, Design and monitoring of an improved test reference environment for the evaluation of BIPV systems, in: Proceedings of the 25th European Photovoltaic Solar Energy Conference, Valencia, Spain, 2010, pp. 5135–5140.
[13] C. Lodi, J. Cipriano, P. Bacher, H. Madsen, Modelling the heat dynamics of a monitored Test Reference Environment for BIPV systems through deterministic and stochastic approaches, in: International Workshop on "Whole Building Testing, Evaluation and Modelling for Energy Assessment", Technical University of Denmark, Lyngby, Denmark, 2011.
[14] IEA ECBCS, Annex 58 Reliable Building Energy Performance Characterisation Based on Full Scale Dynamic Measurements. http://www.ecbcs.org/annexes/annex58.htm.
[15] L. Vandaele, P. Wouters, J.J. Bloem, W.J. Zaaiman, Combined heat and power from hybrid photovoltaic building integrated components: results from overall performance assessment, in: Proceedings of the 2nd World Conference and Exhibition on Photovoltaic Solar Energy Conversion, Vienna, Austria, 1998.
[16] J.J. Bloem, P.H. Baker, Building integration issues for photovoltaics, in: Proceedings of BIAT – Technical Innovation in Design and Contruction, Dublin Castle, 2000.
[17] A. Jager-Waldau, PV STATUS REPORT 2011, JRC Scientific and Technical Reports, European Union, 2011.
[18] J.J. Bloem, P.H. Baker, P.A. Strachan, Energy performance of buildings and the integration of photovoltaics, in: International Conference Improving Energy Efficiency in Commercial Buildings (IEECB'04), Frankfurt, Germany, 2004.
[19] R.P. Kenny, G. Friesen, D. Chianese, A. Bernasconi, E.D. Dunlop, Energy rating of PV modules: comparison of methods and approach, in: Proceedings of the 3rd World Conference on Photovoltaic Energy Conversion, Osaka, Japan, 2003.
[20] J.J. Bloem, W. Zaaiman, C. Bucci, V.R. Nacci, Proposal for a PV reference module and a test reference environment for BIPV applications, in: Proceedings of the 16th European Photovoltaic Solar Energy Conference, Glasgow, UK, 2000.
[21] INIVE EEIG, Stimulating increased energy efficiency and better building ventilation, Brussels, Belgium, 2010, ISBN 2-930471-31-X.
[22] J.J. Bloem, Evaluation of a PV-integrated building application in a well-controlled outdoor test environment, Building and Environment 43 (2008) 205–216.
[23] R.K. Shah, A.L. London, Laminar flow forced convection in ducts, in: Advances in Heat Transfer, Academic, New York, NY, 1978.
[24] F. Incropera, D.P. De Witt, Fundamentals of Heat and Mass Transfer, John Wiley & Sons, New York, 1985.
[25] U. Eicker, Solar Technologies for Buildings, Wiley, Chichester, 2003.
[26] S. Ito, M. Kashima, N. Miura, Flow Control and Unsteady-State Analysis on Thermal Performance of Solar Air Collectors, Journal of Solar Energy Engineering 128 (2006) 354–359.
[27] L.M. Candanedo, A. Athienitis, K.W. Park, Convective Heat Transfer Coefficients in a Building-Integrated Photovoltaic/Thermal System, Journal of Solar Energy Engineering ASME 133 (2011), 021002-1–021002-14.
[28] S. Sharples, Full-scale measurements of convective energy losses from exterior building surfaces, Building and Environment 19 (1984) 31–39.
[29] J.A. Duffie, W.A. Beckman, Solar Engineering of Thermal Processes, 3rd ed., Wiley, 2006.
[30] F.L. Test, R.C. Lessmann, A. Johary, Heat Transfer During Wind Flow over Rectangular Bodies in the Natural Environment, ASME Transactions, Journal of Heat Transfer 103 (1981) 262–267.
[31] J.J. Bloem, R. Versluis, M. Tijssen, W.J. Zaaiman, Thermal modelling and testing results of the reference component, Technical Report PV-Hybrid Pas, JRC Ispra, Italy, 1997.
[32] J. Cipriano, C. Lodi, D. Chemisana, G. Houzeaux, H. Perpiñán, Development and characterization of semitransparent double skin PV facades, in: Proceedings of the 1st International Conference on Solar Heating, Cooling and Buildings, Lisbon, Portugal, 2008.

Please cite this article in press as: J.J. Bloem, et al., An outdoor Test Reference Environment for double skin applications of Building Integrated PhotoVoltaic Systems, Energy Buildings (2012), doi:10.1016/j.enbuild.2012.03.023

Chapter 6: Conclusions and future work

Conclusions and future work

Abstract

In the final chapter the main achievements and conclusions of the work are summarized and prospectives for future research in the field are outlined. Lastly, the publication status of the papers is also included.

1. General discussion and conclusions

Double skin Building Integrated Photovoltaic systems have been developed widely in the past decade, appearing as promising applications for achieving the requirements of the new EU directive on the energy performance of buildings (EPBD). In this work, a contribution to the energy performance assessment of mechanically ventilated double skin BIPV facades is presented by means of testing, analysis and modelling work.

Experimental work was carried out in order to address the need for experimental studies of ventilated double skin BIPV systems under real outdoor conditions. Tests have been carried out over a mechanically ventilated glass-tedlar silicon PV module in the outdoor Test Reference Environment (TRE) located in Lleida. The TRE outdoor test facility allowed testing the selected BIPV system in a well-controlled environment by assessing the impact of different parameters (i.e. airflow rate, inclinations, rear-facing materials) on the active components performance. The duration of the experiments was found to be a 2-day minimum in order to get enough information from data. The experimental evaluation of the system indicated that good workmanship and appropriate design are key elements in achieving the desired performances. A lack of air tightness, poor insulation at the rear-facing surface or an inappropriate choice of the sensors and their protections were identified as the major shortcomings of the design.

Regarding the air gap temperatures, cylindrical shading protections are found the most effective to avoid effects from direct solar radiation over the thermocouples readings. In order to obtain a smoother temperature reading, some thermal mass was given to the sensors by using small copper plates.

Regarding the airflow rate measurements, two different methods were tested and compared, highlighting the complexity of achieving accurate measurements, even when mechanically airflow rate is concerned.

To reduce measurement errors of the global incident solar radiation, it was found very important to place the pyranometer perfectly in line with the PV module and at middle height. Wind direction and speed have been measured with a cup-type anemometer placed next to the TRE and at PV

module level (2 m height); measurements from the weather station placed at 10 m height have been applied for control or back-up purposes only.

The PV module temperature plays an important role in the energy characterization of the system as both the electrical and thermal efficiencies depend on it. The measurements of the PV cells temperature indicate that the horizontal temperature gradient of the PV module is negligible in all configurations (< 1°C). On the other hand, the vertical temperature gradient has to be taken into account, even when a single PV module is concerned, as considerable temperature differences occur between the upper and lower part (up to 10°C).

Two different rear-facing materials have been tested in the TRE with the same PV module: one was a black absorber sheet and the other was a white diffuse reflector. Considering the same level of solar irradiance and similar incidence angles, with the white diffuse reflector the average temperature of the PV module is around 8°C lower than with the black absorber sheet, slightly increasing the average PV cells electrical efficiency (+0.5%). Vertical PV module temperature gradient reduces with the white diffuse reflector at the rear-facing surface, and the PV cells at middle height have almost the same temperature as the PV cells at the top. The thermal efficiency decreases when the deviation from the optimized inclination increases because of the angle dependence of the reflection losses of the PV module. The black absorber sheet improves the thermal production of the system compared to the white diffuse reflector: for the lower airflow rates ($\mathrm{Re} \leq 7000$), the increse in the thermal efficiency goes from 30% to 100% while for the higher airflow rates ($\mathrm{Re} > 7000$), it is approximately 10% higher.

Plots of the average temperature difference between the PV module and the ambient air versus irradiance have revealed that the behavior of each PV module does not follow a straight line in the graph; in particularly, the temperature difference follows two different trends before and after solar midday because of the thermal inertia of the PV modules, which therefore has to be taken into account in the modelling work.

Considerable temperature differences were found between the ventilated PV module and the two reference modules in terms of both electrical efficiency and average module temperature.

System identification techniques have been applied for the energy performance assessment of the tested systems and unknown physical parameters have been identified. The application of these techniques requires a high level of knowledge of physical and mathematical processes. In particular, continuous-discrete stochastic state space grey-box models have been found to be the most appropriate for modelling the heat dynamics of the ventilated BIPV module from the measured data. The strengths of grey-box models are the possibility to combine physical and data driven information in order to identify model parameters and to provide information about uncertainties of the model. The effects due to accumulation of heat or evolution of the variables in time are properly taken into account. Within this study, both one-state and two-state grey-box models have been developed. As considerable temperature differences occur between the upper and lower part of the PV module, it was found preferable to consider two vertical levels for the energy balance of the BIPV system (two-state grey-box model). The most relevant differences with the previous work found in literature is the direct estimation of the convective heat transfer coefficients between

the PV module and the air gap, and the PV module heat capacity. In addition, other physical inputs and outputs are also considered in the presented models: the angular dependency of the optical properties of the PV module, the electricity production, the effect of PV module inclination over the heat transfer coefficients and the consideration of the ground and sky temperatures for the radiative losses calculations.

It has been shown that the two-state model provides the best description of the dynamics of the system and this finding is not contradicted by white noise tests. It has also been shown that the two-state model performs properly both in prediction and simulation context. Considering the energy balances at each energy exchange layer, the assumption of the lumped capacitance method was found acceptable.

Regarding the convective heat transfer coefficient within the air gap, the estimated values with the two-state model are predicted properly with the Ito's relation for transient and turbulent regimes, while in laminar conditions Candanedo's relation approximates quite accurately the estimated Nusselt numbers. Considering the estimated values of the PV module heat capacity, they differ slightly for different Reynolds numbers, especially for lower Reynolds numbers; the differences are not statistically significant for Re $>$3000 and for the lower values the difference could be caused by non-modelled natural convection effects that should be included in more advanced models.

It was found that in order to validate any analysis or modelling work, high quality data are a necessary requirement. A proper check of the measured data for unexpected observations was therefore required and if necessary data were filtered in time and space in order to be used as input signals for analysis. Simple graphical representation of the signals may indicate any inconsistency.

In order to harmonise experimental work for the assessment of electrical as well as thermal characteristics of photovoltaic systems in the building envelope, the Thesis concludes with the definition of a common outdoor Test Reference Environment (see Chapter 5). Two reference mini-modules are proposed to get the required information for evaluation, one fully insulated and one under free-rack condition. These modules give an indication of the BIPV performance range, introducing an additional point, the Insulated Condition Temperature for PV modules. It could be interesting to insert the ICT point into the IEC 61215, which now includes only STC (laboratory conditions) and NOCT (free-rack mounted conditions) points.

It has been found that the evaluation and modelling processes should provide a reciprocal feedback to each other for high quality performance characterisation. In fact, results from evaluation can be an input for model validation work but also modelling work gives input to evaluation for model optimisation and for a proper design of the experimental work. Harmonisation could be further developed in EU projects to support the definition of international standards for ventilated double skin BIPV facades.

2. Future work

Other experiments are recommended to evaluate the effect of other rear-facing materials over the energy balance of the system. Glass-glass BIPV modules could be tested in the TRE to verify the

applicability of the model to other PV module configurations. PV modules with different packaging factors could be tested as well. In addition, by testing other rear-facing materials at the TRE rear-facing surface, the applicability of the presented model for different optical properties of the system could be verified in future work.

An important step towards an overall energy performance assessment would be the integration of the developed model into a whole building model including the HVAC system. This extension will allow evaluating the opportunity to couple the pre-heated air from the ventilated BIPV modules with the HVAC system of the building, improving its efficiency. An intermediate step would be the validation of the developed model with a full-scale building with a double-skin BIPV façade or roof without occupancy.

It would be also interesting to investigate the possibility to study the effect of natural ventilation within the TRE air cavity.

From the statistical evaluation of the developed two-state model, it has been shown that the model may be improved by using the information which is embedded in the diffusion term. In this particular case, it might be interesting to verify whether a possible model improvement would be the introduction of a dependency of the solar radiation or the PV module temperature in the noise term.

In addition, since considerable temperature differences were found between the upper and lower part of the PV module, it is presumed that there is a potential in moving from a two-state to a three-state model by considering three vertical levels for the energy balance of the BIPV system.

3. Publication status of the papers

The Thesis is composed of a series of papers, accepted or to be submitted to international peer-reviewed journals. The actual status of the papers is as follows:

Table 1: Publication status of the papers presented in this Thesis (May 8^{th}, 2012)

Chapter	Journal	Status
2. State of the art		To be submitted
3. Monitoring		To be submitted
4. Modelling	EB*	Accepted, Corrected Proof
5. Standard TRE	EB*	Accepted, Corrected Proof

*** Energy and Buildings, Inprint: ELSEVIER, ISSN: 0378-7788

ANNEX I

Mathematical background of stochastic grey-box models

Parameter estimation and the extended Kalman filter

In general, when a heat transfer process is considered, time and space are normally seen as stochastically independent variables. It is therefore necessary to describe the process with partial differential equations. Since partial differential equations are often complicated to solve, the lumped parameterization method is used to simplify the mathematics. In fact, the method turns the partial differential equation into ordinary differential equations, much easier to handle and solve. Lumped processes are all processes in which the spatial dependence of the variables under consideration can be neglected [1]. Since lumped processes are always approximations of reality, i.e. the physical properties are actually changing in the space dimensions, it is necessary to investigate the applicability if this method in each specific case. The extension from single-state to multiple-state models is a possibility to overcome the problem by taking the spatial variation over one axis into account.

The grey-box models used in this work are continuous time stochastic state space models, which are lumped capacitance models with addition of noise. The evolution in time of the lumped states is described by a set of stochastic differential equations (SDE's) (system equations):

$$dx_t = f(x_t, u_t, t, \theta)dt + \sigma(u_t, t, \theta)d\omega_t \tag{1}$$

which are indirectly observed as described by the set of discrete time measurement equations (measurement equations):

$$y_k = h(x_k, u_k, t_k, \theta) + e_k \tag{2}$$

where $x_t \in \chi \subset \mathbb{R}^n$ is a vector of state variables, $u_t \in \mathcal{U} \subset \mathbb{R}^m$ is a vector of input variables, $t \in \mathbb{R}$ is the time variable, $\theta \in \Theta \subset \mathbb{R}^p$ is a vector of parameters, $y_k \in \mathcal{Y} \subset \mathbb{R}^l$ is a vector of output variables. $f(\cdot) \in \mathbb{R}^n$, $\sigma(\cdot) \in \mathbb{R}^{n\mathtt{x}n}$ and $h(\cdot) \in \mathbb{R}^l$ are known but possibly non-linear functions; $\{\omega\}$ is an n-dimensional standard Wiener process. $\{e_k\}$ is an l-dimensional white noise process with $e_k \in N(0, S(u_k, t_k, \theta))$, and $\sigma(\cdot)$ is the gain of the increments of the Wiener process. Hence the total noise in the model is decomposed into a process noise term (ω_t) and a measurement noise term (e_k) and they are assumed to be mutually uncorrelated. This allows for estimation of unknown parameters from experimental data in a prediction error (PE) setting as opposed to the more commonly used output error (OE) setting [2]. The process noise accounts for: modelling approximations (description of the dynamics, etc..), unrecognized and unmodeled inputs (not considered variables which may affect the system, etc..), and noise in the input measurements. The measurement noise term accounts for noise and drift in the output measurements [3].

The SDE's hold the physical description of the system while the measurement equations represent the data driven part.

The solution to Eq. (1) is a Markov process and unknown parameters of the model in Eq. (1) and (2) can be estimated with e.g. maximum likelihood (ML) or maximum a posteriori (MaP) estimation [4]. The mathematics behind the two methods is quite similar since the maximum

likelihood estimation is a special case of the MaP estimation. In this work only ML estimation is applied therefore it is decided to outline only the theory of the ML estimation. The ML estimation of the unknown parameters is carried out by finding the parameters θ that maximize the likelihood function given a sequence of measurements Y_0, Y_1, ..., Y_{N-1}, Y_N. By introducing the notation:

$$y_N = [Y_0, Y_1, ..., Y_{N-1}, Y_N] \tag{3}$$

the likelihood function is the joint probability density:

$$L(\theta; y_N) = \left(\prod_{k=1}^{N} p(Y_k \mid y_{k-1}, \theta) \right) p(Y_0 \mid \theta) \tag{4}$$

where $p(Y_k \mid y_{k-1}, \theta)$ is a conditional density denoting the probability of observing Y_k given the previous observations and the parameters θ. $p(Y_0 \mid \theta)$ is the probability distribution function (pdf) of the starting conditions.

The maximum likelihood estimates of the parameters are then given by:

$$\hat{\theta} = \underset{\theta}{argmax} \{L(\theta, y_N)\} \tag{5}$$

The covariance matrix is obtained by approximating the Fisher Information matrix with the inverse of the observed Hessian matrix evaluated at the final estimates. The uncertainties of the parameter estimates are obtained by decomposing the covariance matrix into a diagonal matrix of the standard deviations of the parameter estimates and the corresponding correlation matrix [5].

In the presented work (see Part III), the extended Kalman filter (EKF) algorithm is applied to find maximum likelihood estimated of the parameters in the model.

The recursive algorithm of the extended Kalman filter consists of two main categories of equations: prediction and update. The prediction equations predict the state and observations. The update equations update the state predictions with the last measurement.

The prediction equations of the extended Kalman filter of the output variables are expressed by:

$$\hat{y}^i_{k|k-1} = h(\hat{x}^i_{k|k-1}, u^i_k, t^i_k, \theta) \tag{6}$$

$$\hat{R}^i_{k|k-1} = C\hat{P}^i_{k|k-1}C^T + S \tag{7}$$

The residuals are calculated in the innovation equation:

$$\epsilon^i_k = \hat{y}^i_k - \hat{y}^i_{k|k-1} \tag{8}$$

In each iteration of the extended Kalman filter the Kalman gain is estimated. The Kalman gain determines the level of influence of new observations. If the measurement covariance of an observation is large, the Kalman gain will not attach importance to observation, and the updated

state will be approximately the same value as the predicted one. The Kalman gain equation is:

$$K_k^i = P_{k|k-1}^i C^T (R_{k|k-1}^i)^{-1} \tag{9}$$

After estimating the values of the prediction, innovation and Kalman gain equations the mean and the covariance need to be updated applying Eqs. 10 and 11:

$$\hat{x}_{k|k}^i = \hat{x}_{k|k-1}^i + K_k^i \epsilon_k^i \tag{10}$$

$$P_{k|k}^i = P_{k|k-1}^i - K_k^i R_{k|k-1}^i (K_k^i)^T \tag{11}$$

where

$$\hat{x}_{k|k}^i = E\{x_k^i | \mathcal{Y}_k^i, \theta\} \tag{12}$$

$$P_{k|k}^i = V\{x_k^i | \mathcal{Y}_k^i, \theta\} \tag{13}$$

and $\hat{x}_{k|k}^i$is the conditional mean and $P_{k|k}^i$covariance of the state vector.

Aside from the prediction equations of the output variables, also prediction equations for the state variables have to be run through. The state prediction equations are found in Eqs. and. Initial conditions for the extended Kalman filter are $\hat{x}_{t|t_0}^i = x_0^i$ and $P_{t|t_0}^i = P_0^i$. The extended Kalman filter is sensitive to nonlinear effects and therefore it may be necessary to linearize it about the current mean and covariance, equal to the subsampling. This is actually one of the characteristics of the extended Kalman filter. The linearizing of the filter makes it possible to obtain a better approximation, the time interval $[t_k^i, t_{k+1}^i[$ is sub-sampled, $[t_k^i, ..., t_j^i, ..., t_{k+1}^i[$. In Eqs. and the simplified analytical solution to the corresponding linearized propagation equations are presented.

$$\frac{d\hat{x}_{t|j}^i}{dt} = f_0 + A(\hat{x}_t^i - \hat{x}_j^i) + B(u_t^i - u_j^i) \tag{14}$$

$$\frac{dP_{t|j}^i}{dt} = AP_{t|j}^i + P_{t|j}^i A^T + \sigma\sigma^T \tag{15}$$

for $t \in [t_j^i, t_{j+1}^i[$, where the notation:

$$A = \frac{\partial f}{\partial x_t}|_{\hat{x}_{j|j-1}^i, u_j^i, t_j^i}, B = \frac{\partial f}{\partial u_t}|_{\hat{x}_{j|j-1}^i, u_j^i, t_j^i}$$

$$f_0 = f(\hat{x}_{j|j-1}^i, u_j^i, t_j^i, \theta), \sigma = \sigma(u_j^i, t_j^i, \theta)$$

has been applied. The analytical solutions are:

$$\hat{x}^i_{j+1|j} = \hat{x}^i_{j|j} + A^{-1}(\Phi_s - I)f_0 + (A^{-1}(\Phi_s - I) - I\tau_s)A^{-1}B\alpha \tag{16}$$

$$P^i_{j+1|j} = \Phi_s P^i_{j|j}\Phi^T_s + \int e^{As}\sigma\sigma^T e^{A^T s}ds \tag{17}$$

where $\tau_s = t^i_{j+1} - t^i_j$ and $\Phi_s = e^{A\tau s}$, and where:

$$\alpha = \frac{u^i_{j+1} - u^i_j}{t^i_{j+1} - t^i_j} \tag{18}$$

has been introduced to allow assumption of either zero order hold ($\alpha = 0$) or first order hold ($\alpha \neq 0$) on the inputs between sampling instants. Zero order hold is when the value of the input is held constant, while first order hold method estimates a linear interpolation between the inputs.

Adequability and validation of the model

The first step of the model validation is to test the adequability of the estimated parameters. Possible tests are:

- T-test of the parameters, to verify whether a parameter can be rejected by estimating the p-value, i.e. the probability of the parameter being equal to zero;

- check if the interval of possible values previously defined for each parameter is adequate, i.e. comparing the penalty and the objective function and their derivatives;

- analyze the correlation matrix of the estimated parameters, i.e. considering that values up to 0.96 indicate that the values are acceptable [6], while values above 0.96 indicate that the model is overparameterized and one or more parameters have to be removed from the model.

After testing the parameters, the analysis of the residuals has to be carried out. Apart from the model validation, the analysis of the residuals is also useful as an indication of the further improvements of the model for a better description of the data.

The residuals are defined as the difference between the true and the estimated value of the output variable:

$$\epsilon_t(\theta) = Y_t - \hat{Y}_{t|t-1,\theta} \tag{19}$$

If the model is adequate the residuals must be white noise, i.e. random mutually uncorrelated identically distributed stochastic variables with mean value 0 and constant variance σ^2_ϵ[4].

The initial analysis is to *plot the residuals versus time*. This plot may reveal non-stationarities and potential outliers. Another important test is to *plot the residuals versus the most influential variables of the system*. This test is necessary to detect any dependency of these variables in the noise term. When a dependency is detected, a possible improvement could be the introduction of a dependency of these variables in the noise term.

Further analysis of the residuals may be carried out in the time and in the frequency domain.

In the time domain, the most dominant test is to plot the *estimated autocorrelation function (ACF)*, $\hat{\rho}_\epsilon$, with the approximate 95% confidence interval for the time lags. The autocorrelation function represents the correlation between the residuals at current time and the residuals lagged k-time units and it may reveal if some of the variations in data are not described in the model, for instance periodical tendencies. The limits are found at ± 2 standard deviation. The mean and the variance of the autocorrelation are given as:

$$e[\hat{\rho}(k)] \simeq 0; \quad k \neq 0 \tag{20}$$

$$V[\hat{\rho}(k)] \simeq 1/N; \quad k \neq 0 \tag{21}$$

If the residuals are white noise the autocorrelation function is defined as:

$$\rho_\epsilon(k) = \{ \begin{array}{cc} 1 & k \\ 0 & k = \pm 1, \pm 2, ... \end{array} \tag{22}$$

In order to calculate the autocorrelation function, fist the autocovariance function needs to be calculated as follows:

$$\gamma(k) = Cov[X(t), X(t+k)] \tag{23}$$

where $X(t)$ is a stationary process, t is the time indicator and k denotes the time lag. The autocorrelation function is therefore defined as:

$$\rho(k) = \gamma(k)/\gamma(0) \tag{24}$$

The autocovariance function is calculated as:

$$C(k) = \frac{1}{N} \sum_{t=1}^{N-|k|} (Y_t - \overline{Y})(Y_{t+|k|} - \bar{Y}) \tag{25}$$

for $|k| = 0, 1, ..., N-1$. Furthermore, $\overline{Y} = (\sum_{t=1}^{N} Y_t)/N$.

Based on the estimated autocovariance function, the estimated autocorrelation function can be calculated as:

$$\hat{\rho}(k) = r_k = C(k)/C(0) \tag{26}$$

When considering tests in the frequency domain, the *normalized cumulated periodogram (CP)* is used. The CP is the frequency domain representation of the variation of the residuals. This test reveals if there are any specific areas of the frequency domain where the residuals are over-represented, for instance due to seasonal or periodic skew behaviour of the residuals. Since the variation of white-noise residuals is uniformly distributed, no frequency ought to be over-represented. Normally, a

95% limit band is considered in the analysis. A straight line from (0,0) to (0.5,1) inside the limit of the periodogram indicates that the residuals are white noise.

Eq. shows thee calculation of the periodogram of the residuals, $I(v_i)$:

$$\hat{I}(v_i) = \frac{1}{N}[(\sum_{t=1}^{N} \epsilon_t cos2\pi v_i t)^2 + (\sum_{t=1}^{N} \epsilon_t sen2\pi v_i t)^2] \tag{27}$$

where $v_i = \frac{i}{N}$ are the frequencies, $i = 0, 1, ..., N/2$ and N denotes the total number of observations. $\hat{I}(v_i)$ is the amount of variation of ϵ_t related to the frequency v_i. The normalized periodogram is:

$$\hat{C}(v_j) = [\sum_{i=0}^{j} \hat{I}(v_i) / \sum_{i=0}^{\frac{N}{2}} \hat{I}(v_i)] \tag{28}$$

The confidence limits for the periodogram are calculated by $\frac{\pm K_\epsilon}{\sqrt{q}}$, where $q = \frac{n-2}{2}$ for n even and $q = \frac{n-1}{2}$ for n odd. The approximated coefficient K_ϵ for the probability limit 5% is 1.36.

References

[1] V. Kecman, *State-space Models of Lumped and Distributed System.* Springer-Verlag ed., 1988.

[2] M. Jimenez, H. Madsen, J. Bloem, and B. Dammann, "Estimation of non-linear continuous time models for the heat exchange dynamics of building integrated photovoltaic modules," *Energy and Buildings*, vol. 40, pp. 157–167, 2008.

[3] H. Madsen, J. Holst, and E. Lindstrom, *Modelling Non-linear and Non-stationary Time Series.* IMM,DTU, 2007.

[4] H. Madsen, *Time series analysis.* New York: Chapman and Hall/CRC, 2008.

[5] H. Madsen and P. Thyregod, *Introduction to General and Generalized Linear Models.* CRC press ed., 2010.

[6] N. Friling, *Stochastic modelling of building integrated photovoltaic modules.* Master's thesis, Informatics and mathematical modelling, Technical University of Denmark, 2006.